

NASA CR-179630
June 24, 1987

STUDY OF OPTOELECTRONIC SWITCH FOR SS-TDMA
Final Report

S. F. Su, L. Jou, and J. Lenart

Contract No. NAS3-24673

Submitted to:
NASA/Lewis Research Center
21000 Brookpark Road
Cleveland, OH 44135

GTE Laboratories Incorporated
Waltham, MA 02254

1. Report No. NASA CR-179630	2. Government Accession No.	3. Recipient's Catalog No.
4. Title and Subtitle STUDY OF OPTOELECTRONIC SWITCH FOR SATELLITE-SWITCHED TIME-DIVISION MULTIPLE ACCESS	5. Report Date	6. Performing Organization Code 650-60-26
7. Author(s) SHING-FONG SU, LIZ JOU, AND JOE LENART	8. Performing Organization Report No.	10. Work Unit No.
9. Performing Organization Name and Address GTE LABORATORIES, INCORPORATED 40 SYLVAN ROAD WALTHAM, MASSACHUSETTS 02254	11. Contract or Grant No. NAS-24673 NAS3-24673	13. Type of Report and Period Covered CONTRACTOR REPORT
12. Sponsoring Agency Name and Address NASA LEWIS RESEARCH CENTER 21000 BROOKPARK RD. CLEVELAND, OHIO 44135	14. Sponsoring Agency Code	
15. Supplementary Notes		
16. Abstract <p>The use of optoelectronic switching for SS-TDMA will improve the isolation and reduce the crosstalk of an IF switch matrix.</p> <p>This report presents the results of a study on optoelectronic switching. Tasks include literature search, system requirements study, candidate switching architectures analysis, and switch model optimization.</p> <p>The results show that the power-divided and crossbar switching architectures are good candidates for an IF switch matrix.</p>		
17. Key Words (Suggested by Author(s)) OPTOELECTRONIC SWITCHING SPACE-DIVISION SWITCHING SWITCHING ARCHITECTURES WIDEBAND/BROADBAND SWITCHING	18. Distribution Statement GENERAL RELEASE	
19. Security Classif. (of this report) UNCLASSIFIED	20. Security Classif. (of this page) UNCLASSIFIED	21. No. of Pages 1
		22. Price*

* For sale by the National Technical Information Service, Springfield, Virginia 22161

NASA-C-168 (Rev. 10-75)

OPTOELECTRONIC SWITCHING
SPACE-DIVISION SWITCHING
SWITCHING ARCHITECTURES
WIDEBAND/BROADBAND SWITCHING

OPTOELECTRONIC SWITCHING
SPACE-DIVISION SWITCHING
SWITCHING ARCHITECTURES
WIDEBAND/BROADBAND SWITCHING

"EXECUTIVE SUMMARY"

NASA Executive Summary

Current satellites use FETs, couplers, and other semiconductor devices for an IF NxN switch matrix. Isolation between ON- and OFF-states will degrade and crosstalk between input and output lines of this electronic switch matrix will increase at high operation frequencies. These will impose limitations on the use of an electronic switch matrix for future broadband satellite switching service.

One way to achieve a high-speed, low-crosstalk, and high-isolation electrical switching is to use an optoelectronic matrix switch.

A study on optoelectronic switching techniques for an SS-TDMA was conducted. A summary of the study is presented below:

LITERATURE SEARCH

A literature search indicated that optoelectronic devices have received extensive studies during the past ten years; however, the system concepts and architectures in optoelectronic switching have not attracted adequate attention.

SYSTEM REQUIREMENTS FOR SS-TDMA

- Dynamic interconnectivity between the uplink and downlink beams.
- Capability of one-to-one, one-to-many, and broadcasting connections.
- Switch size of 20x20 with expandability to 100x100.
- High switching speed (< 10 ns), low power consumption, low crosstalk, high isolation, and small physical size.
- High reliability and long lifetime (> 10 years).
- Redundancy embedded in the switch.

- Ability to withstand outside perturbations.

GaAs WIDEBAND/BROADBAND SWITCHING TECHNOLOGY

GaAs FETs can meet the switching speed, isolation, and insertion loss requirements of an IF switch matrix. However, in a GaAs switch matrix, crosstalk exists not only among output lines but also among input lines and between input and output lines. The crosstalk increases as the operation frequency and switch matrix size increase. A reported simulation result indicates that the crosstalk will be higher than -20 dB when the switch matrix size is larger than 8x8.

OPTOELECTRONIC SWITCHING ARCHITECTURES

Optoelectronic switching employs a photodetection process to perform the switching function and is applicable for either analog broadband switching or high-bit-rate digital switching.

Major advantages: Low crosstalk and high isolation.

Capability:

- Switching speed -- 10 to 100 ps.
- Crosstalk -- less than -80 dB (among input lines and between input and output lines).
- Isolation -- better than 70 dB at 4 GHz
- Switch matrix size -- 20x20 (hybrid integration), 4x4 (monolithic integration today), 20x20 (monolithic integration two years from now)
- Insertion loss -- less than 18 dB.
- Total power dissipation -- less than that of an electronic switch of comparable size.

Candidate switching architectures: Power-divided and crossbar switching architectures are good candidates for an SS-TDMA IF switch matrix.

SYSTEM COMPONENTS

System components include optical sources, fiber couplers, optical waveguides, and photodetectors.

Optical sources: A variety of LEDs and laser diodes are available for application in an optoelectronic switch. Laser diodes are preferred because they offer:

- Narrow emission spectra (< 2 nm).
- Wide modulation bandwidth (> 2 GHz).
- Efficient coupling into fibers (about 50% in coupling efficiency).

Fiber couplers: There are two types of optical couplers: passive fiber couplers and active optical couplers.

Photodetectors: PIN photodiodes, avalanche photodiodes, Schottky barrier photodiodes, and photoconductors have a frequency response up to tens of GHz. These devices are widely used in optical communication systems. Photoconductors are the most suitable devices for IF switch applications because they offer low power consumption and compatibility with electronics.

SWITCH MODELS AND OPTIMIZATION

Three switch models are presented: discrete-component, hybrid-integrated, and monolithic-integrated switch models. The discrete-component switch model is useful for proof-of-concept, but hybrid-integrated and monolithic-integrated switch models are good candidates for SS-TDMA switch implementations.

The key to optimize a discrete-component or a hybrid-integrated switch matrix is to reduce the excess loss of the fiber couplers. Realization of an optimum monolithic-integrated switch matrix will require improvements in integration technology.

SYSTEM ADVANTAGES OF OPTOELECTRONIC SWITCHING

The major advantages of optoelectronic switching systems include high isolation, low crosstalk, small physical size, light weight, and low power consumption. Monolithic integration is preferable to fully exploit these advantages.

Technology needed for monolithic optoelectronic switching:

To be monolithically integrated with other elements, the laser diodes are required to have a low threshold current, a low temperature sensitivity, a stable single-mode operation, and a high modulation speed.

For optical detection, a planar structure photodetector is desirable for monolithic integration with other electronic circuits. Horizontal integration is preferred for optoelectronic integrated circuits because it offers lower capacitive coupling between the devices.

To achieve the above goals, improvements in the integration technologies for lasers, photodetectors, and transistors are needed.

Future optoelectronic integrated circuit technology:

Future optoelectronic integrated circuit technology must not only refine existing technology but also explore novel functions and structures. To this end, the multi-quantum well structure is considered to be the leading technology for future optoelectronic switching systems.

"REPORT SUMMARY"

This report presents the results of the NASA Contract NAS3-24673, "Study of optoelectronic switch for SS-TDMA". Included are a bibliography of applicable literature, a study of system requirements, an analysis of candidate architectures, optimization of switch models, and a discussion of the advantages of the optoelectronic switch.

A literature search indicates that optoelectronic devices and their physical phenomenon have been extensively studied and published during the past ten years. However, relatively few papers have addressed the system concepts and architectures in optoelectronic switching.

System requirements for SS-TDMA are studied by considering the functionality, survivability, and reliability of the on-board satellite switch. System requirements for electronic switch matrices are documented in the NASA reports [1-3]. These system requirements are used as a basis for this study of optoelectronic switch matrices.

Recent progress in electronic wideband/broadband switch matrices based on GaAs IC technology is up-dated and a projection of the switching capability that can be developed within the next two years is discussed.

Optoelectronic switching employs a hybrid optical/electronic principle to perform the switching function and is applicable for either analog broadband switching or high-bit-rate digital switching. A number of optoelectronic switching architectures are explored: power-divided, crossbar, optical-coupled, and holographic switch architectures. Detailed studies of these switching architectures indicate that the power-divided and the crossbar switch architectures are good candidates for an SS-TDMA IF switch matrix.

System components including optical sources, optical couplers, and photodetectors are studied in detail. Our study shows that laser diodes, optical couplers, and photoconductors are good candidates for serving as light sources, light distribution paths, and photodetectors, respectively. Laser diodes are better than LEDs for light sources because laser diodes can be modulated at higher frequencies and have a higher optical power. Ei-

ther passive fiber couplers or active optical couplers can be used for light distribution. Photoconductors are chosen for light detection because they are easy to fabricate, compatible with FETs and low in bias voltage.

Performance of the crossbar and power-divided switching architectures are evaluated based on crosstalk, isolation, insertion loss, matrix size, drive power, throughput, and switching speed. Crosstalk is a function of operation frequency, package parasitic reactances, and characteristics of the photodetectors. Isolation depends on operation frequency and noise levels of the photodetectors. Insertion loss is determined by the switching architectures, the switch matrix size, and the type of couplers used. The maximum switch matrix size that can be constructed depends on laser power, photodetector sensitivity, coupler excess loss, coupler splitting ratio, and switching architecture. Power dissipation of a switch matrix is a function of laser driving power, switch matrix size, and excess loss of the couplers. Throughput is a function of switch matrix size and modulation frequency of the lasers. Switching speed depends on the photodetectors used and the switch matrix structure (discrete or integrated).

Three switch models are proposed based on the performance analysis: discrete-component, hybrid-integration, and monolithic-integration switch models.

System advantages and disadvantages of optoelectronic switches are evaluated. Some crucial factors in optoelectronic integration are examined. A comparison of hybrid integration with monolithic integration is also made.

Monolithic integration is preferable to fully exploit the system advantages of optoelectronic switching. To this end, multi-quantum well structures are predicted to be the leading technology for future optoelectronic switching systems.

CONTENTS

"EXECUTIVE SUMMARY"	2
"Report Summary"	6
<i>Chapter</i>	<i>Page</i>
1. INTRODUCTION	1
2. A BRIEF REVIEW OF SS-TDMA SYSTEMS	2
2.1 Operation of SS-TDMA systems	2
2.2 Reference System Requirements for SS-TDMA	3
3. GaAs WIDEBAND/BROADBAND SWITCHING TECHNOLOGY	5
3.1 Recent Progress in GaAs IC Technology	5
3.2 Capability of GaAs Wideband/Broadband Switching Technology	7
4. OPTOELECTRONIC SWITCHING	10
4.1 Operation Principle of an Optoelectronic Switch Matrix	11
4.2 Advantages of Optoelectronic Switching	12
4.3 Performance Requirements for an Optoelectronic Switch Architecture	13
4.4 Capability of Optoelectronic Switching	14
4.5 Optoelectronic Switching Architectures	16
4.6 Feasibility of Employing Optoelectronic Switching Architectures in an IF Switch	24
4.7 Modularity of the Candidate Switching Architectures	24
5. SYSTEM COMPONENTS	26
5.1 Optical Sources	26
5.1.1 Basic Operation and Device Structures of a Laser Diode	26
5.1.2 Advantages and Disadvantages of Laser Diodes	28
5.1.3 Material and Output Characteristics of Laser Diodes	29
5.1.4 Modulation of Lasers	30
5.1.5 Selection of Laser Diodes	32
5.2 Couplers	33
5.2.1 Passive fiber couplers	33
5.2.2 Active Optical Couplers	34
5.3 Photodetectors	36
5.3.1 PIN Photodiodes	36
5.3.2 Avalanche Photodiodes	37
5.3.3 Schottky Barrier Photodiodes	38
5.3.4 Photoconductors	39
6. PERFORMANCE EVALUATION OF THE SWITCHING ARCHITECTURES	41
6.1 Crosstalk	41
6.2 Isolation	42
6.3 Insertion Loss	42
6.4 Switch Matrix Size and Throughput	43
6.5 Power Dissipation	43

6.6 Switching Speed	44
7. SWITCH MODELS AND OPTIMIZATION	45
7.1 Discrete Component Switch Model	45
7.2 Hybrid Integration Switch Model	46
7.3 Monolithic Integration Switch Model	47
7.4 Optimization of the switch models	49
8. ADVANTAGES AND DISADVANTAGES OF OPTOELECTRONIC SWITCHING SYSTEMS	50
8.1 Comparison of Monolithic optoelectronic and GaAs MMIC switches	50
8.2 Technology needed for monolithic optoelectronic switching	51
8.3 Future Optoelectronic integrated circuit technology	53
9. CONCLUSIONS AND RECOMMENDATIONS	54
9.1 Conclusions	54
9.2 Recommendations	55
10. REFERENCES	57

Chapter 1

INTRODUCTION

Current satellites use FETs, couplers, and other semiconductor devices for an IF $N \times N$ switch matrix. Isolation between ON- and OFF-states will degrade and crosstalk between input and output lines of this electronic switch matrix will increase at high operation frequencies. These will impose limitations on the use of an electronic switch matrix for future broadband satellite switching service.

One way to achieve a high-speed, low-crosstalk, and high-isolation electrical switching is to use an optoelectronic matrix switch.

This report presents the results of the NASA Contract NAS3-24673, "Study of optoelectronic switch for SS-TDMA". A review on SS-TDMA system requirements is given in Chapter 2. Recent progress and a projection of future developments in GaAs switching technology are presented in Chapter 3. Studies of optoelectronic switching technologies are described in Chapter 4. In Chapter 5, system components (laser diodes, optical couplers, and photodetectors) are evaluated. Switching architectures and their performance are discussed in Chapter 6. Proposed switch models and their optimizations are presented in Chapter 7. In Chapter 8, optoelectronic and GaAs IC switches are compared.

Chapter 2

A BRIEF REVIEW OF SS-TDMA SYSTEMS

2.1 OPERATION OF SS-TDMA SYSTEMS

Satellite Switched Time Division Multiple Access (SS-TDMA) is a technique combining satellite switching and TDMA concepts to enhance the bandwidth utilization. In an SS-TDMA system, the TDMA information bursts of uplink beams are rapidly and accurately connected to the designated downlink destinations by the on-board satellite switch. Figure 1 shows a simplified example of an SS-TDMA system containing three terminals. Each terminal consists of a transmitting station and a receiving station. Each transmitting station can transmit traffic bursts to each downlink beam via the on-board satellite switch during an assigned epoch in the TDMA frame. The switch state (or switch configuration) changes for different epoches in a frame. In general, if there are N beams, a total of $N!$ different switch states is required to achieve a complete interconnectivity. (For detailed descriptions on SS-TDMA see NASA documents [1,2,3].)

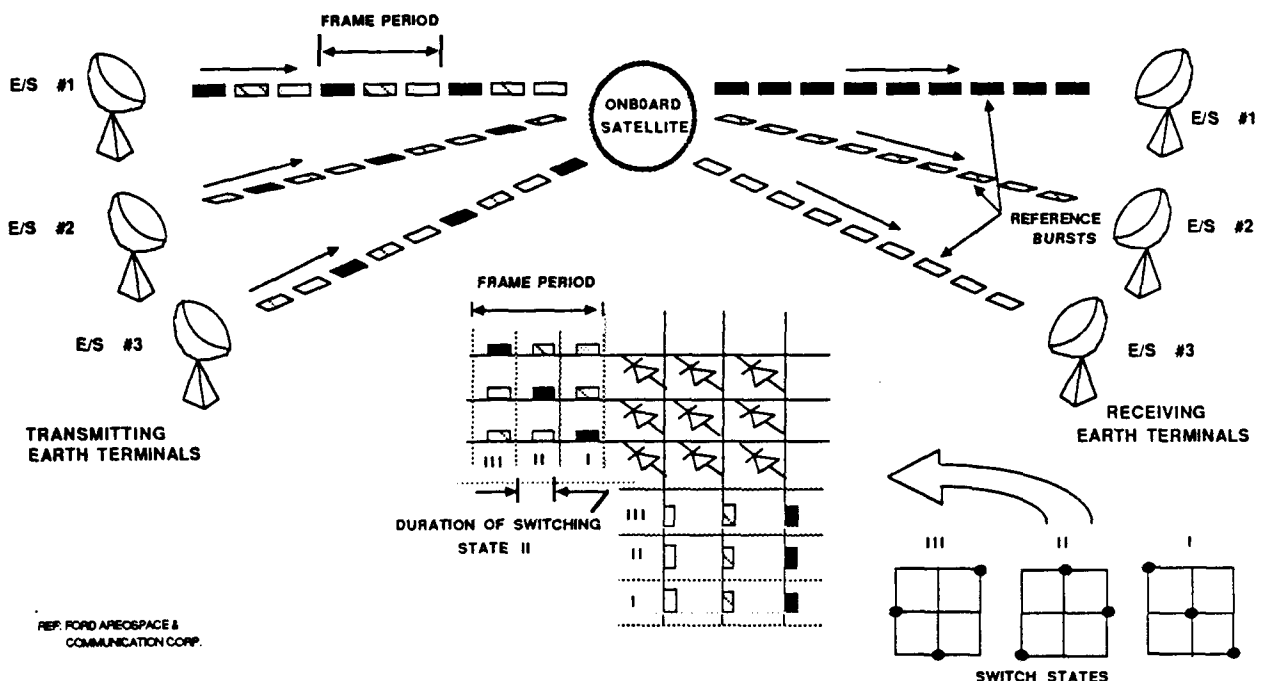


Fig. 1. Satellite-switched time division multiple access (SS-TDMA).

A reference satellite routing system is shown in Fig. 2. There are two major switches in this system, the baseband switch and the IF switch. The major function of the baseband switch is to provide interconnectivity and channel(s) selection of the scanning beams. The throughput requirement for the baseband switch is about 2 GHz. Its control functions are rather complicated. As for the IF switch, the required throughput is about 4 GHz. But, its control functions are relatively "dumb" (i.e. still can make decision on how information should be routed but with minimal intelligence).

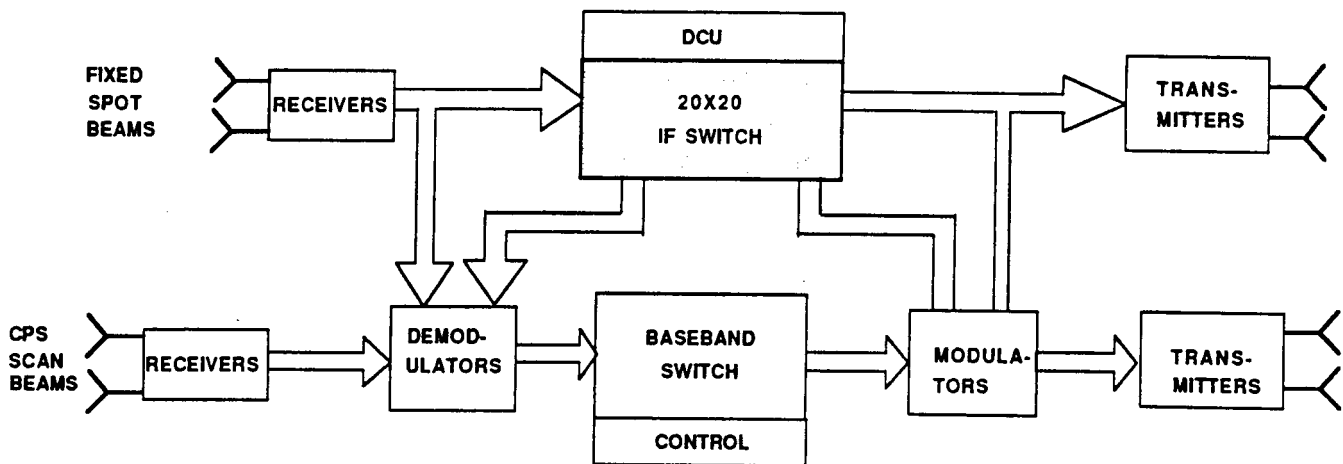


Fig. 2. SS-TDMA transponders.

2.2 REFERENCE SYSTEM REQUIREMENTS FOR SS-TDMA

The system requirements for an SS-TDMA system as stated in Refs. 1-3 are:

- The IF switch must be capable of demonstrating high-speed switching and dynamic interconnectivity between the uplink and downlink beams.
- The switch matrix shall provide one-to-one, one-to-many, and one-to-all (broadcasting) connections.

- The size of the IF switch matrix should be 20 x 20 with expandability to 100 x 100.
- The switching elements must have a high switching speed, a low power dissipation, a low insertion loss, a high isolation, and be small in physical size.
- The lifetime of the switch should be 10 years or longer.
- Redundancy must be embedded in the switch matrix to provide alternative signal paths.
- The switch matrix shall withstand those mechanical, thermal, electromagnetic, vacuum, and radiation stresses in various environments.

Major parameters for the IF switch requirements are listed in Table 1. (For NASA P-O-C specified parameters see Ref. 1).

Table 1. IF switch matrix parameters requirements
(After Ref. 1).

Parameters	Requirements
IF Center Frequency	3.0 - 8.0 GHz
IF Bandwidth	2.5 GHz
Switching Speed	10 ns
Reconfiguration Rate	2 μ s
Isolation	40 dB
Insertion Loss	18 dB

Chapter 3

GAAS WIDEBAND/BROADBAND SWITCHING TECHNOLOGY

Switch devices have been well developed in the electronic domain. PIN diodes, Schottky diodes, and FETs are good candidates for high-speed switching applications (Table 2). GaAs FETs in particular have been considered for wideband/broadband switching applications since the late seventies [4-6]. In this chapter we will up-date the recent progress in GaAs IC technology and discuss the capability of GaAs wideband/broadband switching technology. A projection of the switching capability of GaAs within the next two years will also be discussed.

Table 2. High-speed switching devices.

Type	Switching Speed Capability	Highest Nominal IF Frequency (GHz)
PIN Diode Switch	0.7-5 nsec	20
Schottky Barrier Diode	0.5-5 nsec	30
Bipolar Transistors		
Saturated	>100 nsec	4
Nonsaturated	0.7-50 nsec	4
Field Effect Transistors:		
JFET	< 200 psec	2
Vertical FET	X	X
MESFET(Single Gate)	0.05-1 nsec	20
MESFET(Dual Gate)	0.2-2 nsec	12
Transferred Electron Devices(TEDs)	< 20 psec	30
Josephson Junction Device	< 10 psec	100

3.1 RECENT PROGRESS IN GAAS IC TECHNOLOGY

The progress made in GaAs integrated circuits over the past few years is extremely impressive. GaAs ICs have been extensively utilized for microwave and high-frequency low-noise amplifiers and for high-speed digital applications. The initial work, done on buff-

ered FET logic, demonstrated the high speed capability of GaAs digital circuits at the expense of rather high power dissipation. Later developments in fabrication technology have significantly reduced power dissipation without sacrificing speed and have opened up a new chapter in the realm of high speed digital circuits. Today, GaAs ICs have been used in many digital systems, such as switches [7], shift registers [8], and static RAMs [9-12]. GaAs technology is also being considered for future computer applications. It is predicted that by 1990, a performance of 100 MIPS (Million Instructions Per Second) with a system delay of 200 ps per gate will be required [13]. Silicon-based technology may have difficulty achieving these values. It is also projected that GaAs MESFETs will offer an end-to-end system delay of less than 200 ps at 10 kilogate integration, and HEMT can offer even shorter system delays at the same integration level [13].

In the area of integration, GaAs technology has reached the 4K SRAM complexity level [11,12], which is equivalent to 26,000 devices per chip, and has entered the VLSI realm. However, GaAs VLSI is still at its infancy. Figure 3 shows the progress of GaAs circuit integration during the past 16 years and the projected achievements in the next few years [14]. It is expected that a 64K SRAM will be available in 1988. With today's ever-increasing research and development in GaAs technology [15], full realization of GaAs VLSI should not be far away.

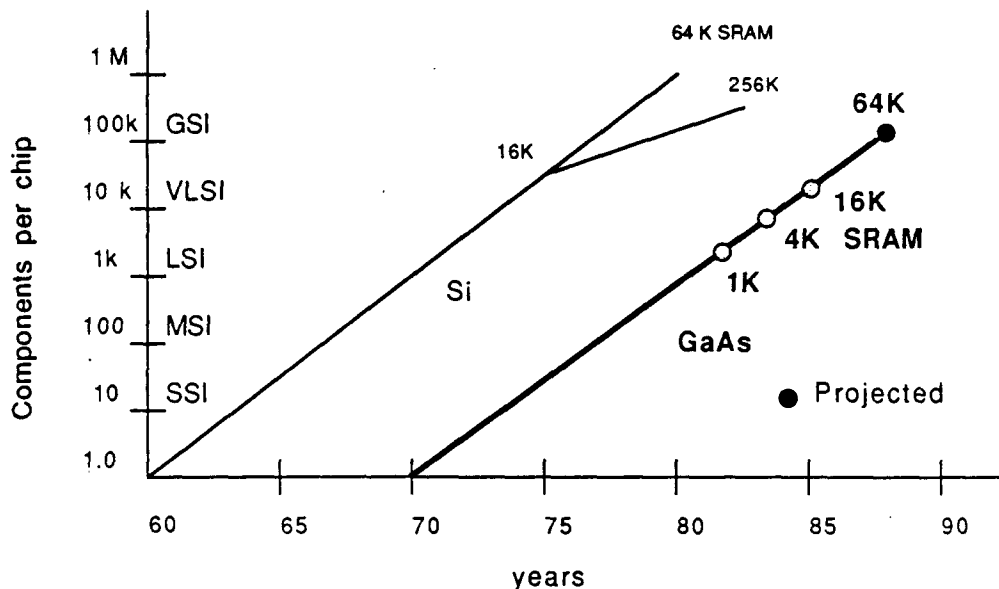


Fig. 3. Progress and projection of Si and GaAs (After Ref. 14).

3.2 CAPABILITY OF GAAS WIDEBAND/BROADBAND SWITCHING TECHNOLOGY

The performance of GaAs FET switches depends heavily on the material quality and the fabrication techniques. The capability of GaAs wideband/broadband switching technology can be assessed by examining the switching speed, switch matrix size, isolation, crosstalk, insertion loss, weight, and total power dissipation. Each of these parameters is discussed below:

A. Switching Speed

The switching speed of a GaAs FET is limited by its propagation delay. In general, GaAs FETs have switching speeds ranging from 10 ps to 100 ps [16]. These switching speeds will satisfactorily meet the switching speed requirement of an IF switch matrix. However, performance of a GaAs FET cannot be measured by looking at the switching speed alone; the speed-power (power-delay) product must also be considered. Unfortunately, these two parameters are always tradeoffs. For example, a minimum delay of 72 ps with a power-delay product of 139 fJ and a minimum power-delay product of 36 fJ with a propagation delay of 157 ps were reported for a GaAs MOSFET [17]. A more detailed discussion on this tradeoff can be found in Ref. 18. So far, many GaAs technologies [6,13,19-23] have already been developed; each with a common goal of trying to improve the switching speed, power dissipation, and integration level. Current data on switching speed and power dissipation per gate for various GaAs ICs are listed in Table 3.

Table 3. Switching speed and power dissipation per gate for various GaAs ICs.

GaAs IC Technology	Switching Speed	Power	Power Delay Product
MESFET BFL	110 ps	40 mW	4.4 pJ
SDFL	110 ps	2.5 mW	0.28 pJ
DCFL	10 ps	0.29 mW	2.9 pJ
JEFET (E-mode)	40 ps	0.1 mW	4 pJ
MOSFET	72 ps	1.93 mW	139 fJ
	157 ps	0.23 mW	36 fJ
HJFET	40 ps	0.4 mW	16 fJ
MODFET	10 ps	1.1 mW	11 fJ

B. Switch Matrix Size

The switch matrix size depends on the number of devices and the associated circuits that can be integrated monolithically. For example, a 4x4 GaAs monolithic switching circuit composed of a switching cell array, decoders, output buffers, and internal bias sources has recently been developed by Nakayama et al. [24]. With today's GaAs integration capability, a 16x16 or 20x20 monolithic switch matrix can be fabricated. Continual progress in GaAs VLSI may make it possible to develop larger GaAs monolithic switch matrices within the next two years.

C. Isolation

Isolation between "ON" and "OFF" states required for NASA's IF switch matrix is 40 dB. This requirement can easily be achieved by today's GaAs technology. For example, the 4x4 monolithic GaAs switch developed by Nakayama [24] has an ON/OFF ratio of 40 dB. More recently, an isolation of 57 dB at 4 GHz has been demonstrated in a 3x3 monolithic GaAs switch. Improvements in GaAs material quality and GaAs fabrication technology may result in even higher isolation.

D. Crosstalk

For monolithic GaAs switch matrices, crosstalk among input channels, among output channels, and between input and output channels is a major problem to be overcome in high-frequency operations. This crosstalk problem may prevent GaAs ICs from being integrated into a large switch matrix. For example, it was reported that the crosstalk will increase from -28 dB for a 4x4 GaAs switch matrix to -18 dB for an 8x8 switch matrix [24]. We do not expect that this problem can be completely solved within the next two years.

E. Insertion Loss

The insertion loss specified for an IF switch matrix is 18 dB. This can easily be achieved by using today's GaAs technology. A broadband GaAs FET 2x1 switch developed by Tajima et al. [25] has a measured insertion loss of less than 8 dB for the frequency range of 0 - 20 GHz.

F. Weight

In the NASA P-O-C model, the weight for an IF switch matrix with 76 crosspoints is 8.685 Kg. If the switch matrix is scaled up to 10,000 crosspoints (100 x 100 switch matrix), the weight of the switch matrix would be more than one ton. This seems too heavy to be economical. Use of monolithic GaAs technology can reduce the weight dramatically.

G. Total Power Dissipation

Low power dissipation per gate is very important to any large-scale circuit technology. In general, the maximum allowable power dissipation in a VLSI chip is 1 W/cm^2 . The 4x4 monolithic GaAs switch mentioned above has a total power dissipation of 1.1 W. It is obvious that power dissipation needs to be improved if large switch matrices are to be constructed.

Chapter 4

OPTOELECTRONIC SWITCHING

There are three basic schemes of optoelectronic switching (Fig 4). The first scheme is transmission path switching (Fig. 4a). The switching is achieved by focusing the controlling laser pulses on a photosensitive path in the switch, changing the resistance of the photosensitive region. Figure 4b shows the oscillator switching technique in which the oscillations of a solid state microwave source are excited, enhanced, or quenched by the controlling laser pulses. The third technique is detector switching (Fig. 4c). The switching is achieved by controlling the biases of the photodetectors. This is the optoelectronic switching technique we will discuss in this chapter.

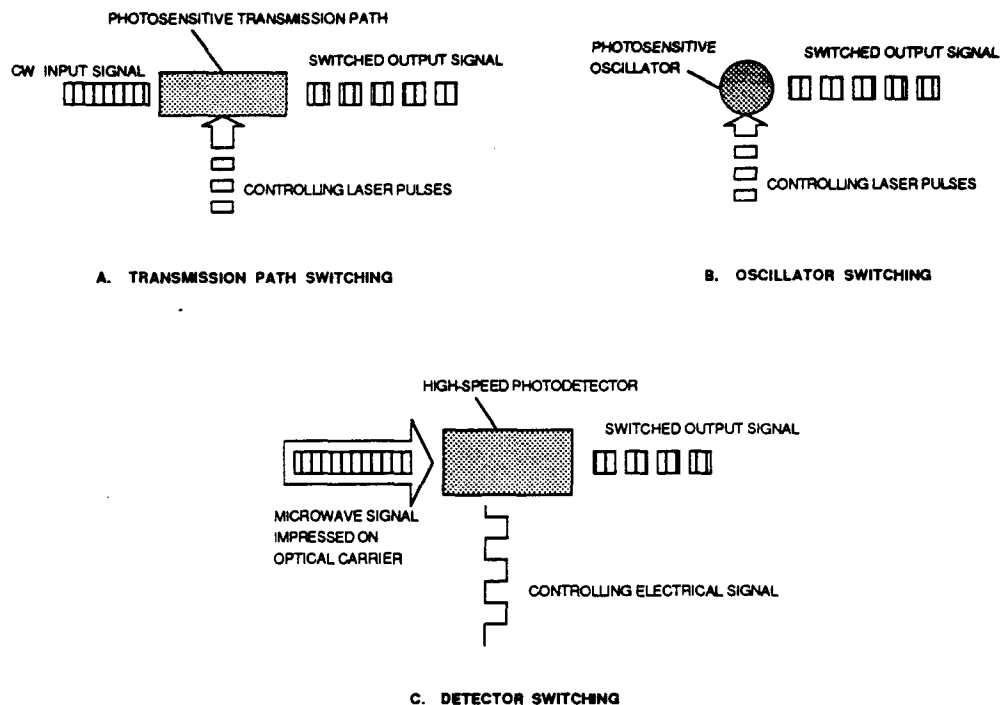


Fig. 4. Three basic types of optoelectronic microwave switching.

Optoelectronic switching was first proposed by MacDonald and Hara for CATV broadband services [26]. During the past few years, research on optoelectronic switching has been very active [27].

Today, optoelectronic switching is finding its way into many application areas. These applications range from large-scale switching of VHF or UHF signals to advanced signal switching functions in high rate digital or high capacity analog channels. Optoelectronic switching technique for SS-TDMA systems is also a good application. In an SS-TDMA system, a communication satellite acts as a switch board connecting the uplink beams to the designated downlink beams. An optoelectronic switch matrix on board the satellite is capable of performing such connections. In this chapter, we will: (1) describe the operation principle of an optoelectronic switch matrix, (2) discuss the advantages of optoelectronic switching, (3) develop a set of performance requirements for an optoelectronic switch architecture, (4) evaluate the capability of optoelectronic switching, (5) explore various types of optoelectronic switching architectures, (6) study the feasibility of employing the optoelectronic switching architecture in an SS-TDMA system, and (7) discuss the modularity of the candidate switching architectures.

4.1 OPERATION PRINCIPLE OF AN OPTOELECTRONIC SWITCH MATRIX

Optoelectronic switching employs a hybrid optical/electronic principle to perform the switching function. Here we will describe the operation principle of a switch matrix only. The physical mechanisms of the switch elements within a switch matrix will be discussed in Chapter 5. In an optoelectronic switch matrix, the incoming electrical signals modulate the light sources (e.g. LEDs or laser diodes). The optical signals from the light sources are distributed to the crosspoints (photodetectors) along fixed optical paths. At the crosspoints, the optical signals are converted to electrical signals. The electrical signals from the photodetectors are then combined to form output lines. The switching function at the crosspoints is accomplished by the photodetection process. Any of the input signals can be made to appear at any output line(s) by rendering the corresponding photodetector(s) sensitive to the optical signals. Figure 5, as an example, shows an $M \times N$ optoelectronic

switch matrix using p-i-n diode crosspoints. The optical signals from the laser diodes enter the switch matrix and are distributed to the p-i-n diodes along the rows. The output electrical signals from the p-i-n diodes are summed up along the columns to form the output lines. The switching function can be accomplished by controlling the biases of the p-i-n diodes. The p-i-n diode switch is on (off) when it is reverse (forward) biased.

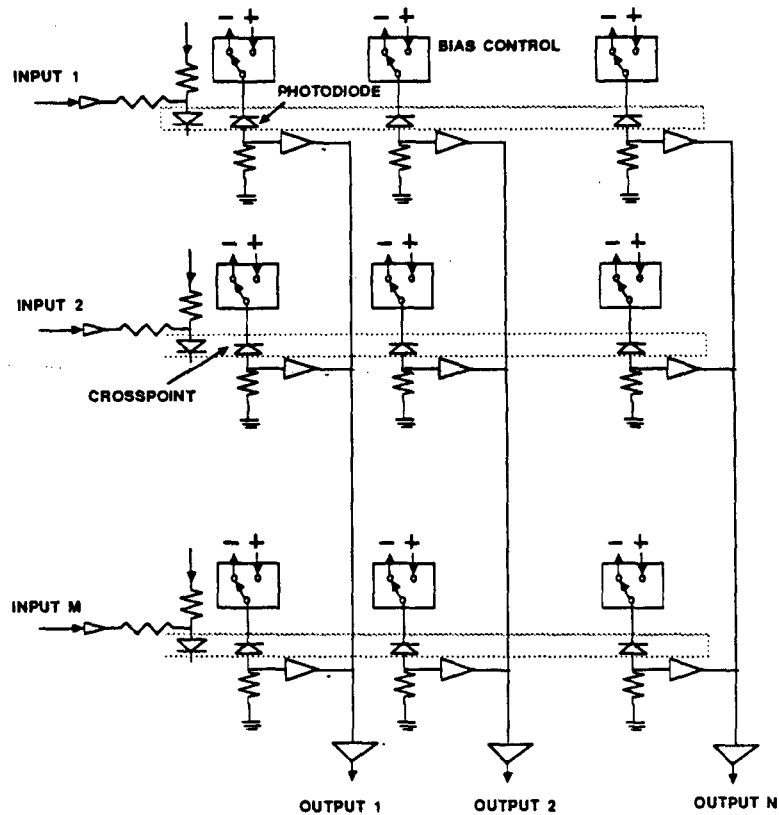


Fig. 5. An MXN optoelectronic switch matrix.

4.2 ADVANTAGES OF OPTOELECTRONIC SWITCHING

An optoelectronic switch matrix has two major advantages over an electronic switch matrix for switching wideband/broadband signals: low crosstalk and high isolation.

A. Low Crosstalk

In an electronic switch matrix, it is very difficult to prevent electromagnetic coupling among electrical lines and through crosspoint switches when high-frequency signals are to

be switched. There is always some crosstalk among the input lines, between the input and output lines, and among the output lines. In an optoelectronic switch matrix, the incoming signals are optical. By nature, photons do not interact with each other and do not couple with electrons. Therefore, there is no crosstalk among the input lines. The crosstalk between input and output lines is through a residual photoresponse of the photodetector at "OFF" state.

B. High Isolation

Isolation in an optoelectronic switch matrix is defined as the ratio of the photodetector output power at ON state to that at OFF state. An isolation better than 70 dB at frequencies up to 1.3 GHz has been demonstrated [28] using photoconductors as the cross-point photodetectors. Calculations also indicate that an isolation of 70 dB can be achieved at frequencies up to 4 GHz. In addition, there are no transient optical reflections from the photodetectors because the electrical state of the photodetector does not affect its optical state significantly. Therefore, switching transients that might disturb other output lines are not produced in an optoelectronic switch matrix.

A detailed comparison between a specific optoelectronic switch architecture and a GaAs IF switch model will be addressed in Chapter 8.

4.3 PERFORMANCE REQUIREMENTS FOR AN OPTOELECTRONIC SWITCH ARCHITECTURE

To be useful for SS-TDMA IF switch applications, an optoelectronic switching architecture must meet the following requirements:

- The switch matrix must be able to operate at frequencies from 2 to 10 GHz.
- Switching speed must be faster than 10 ns.
- Isolation must be higher than 40 dB.
- End-to-end insertion loss must be less than 18 dB.
- Reconfiguration rate must be less than 2 μ s.

- The switch matrix must be able to provide one-to-one, one-to-many, and one-to-all (broadcast) connectivities.
- The switch matrix size should be 20 x 20 with expandability to 100 x 100.
- The switch matrix must have a lifetime of over 10 years.
- The optoelectronic switch components must be space qualified.
- The switch matrix must be able to withstand mechanical, thermal, electromagnetic, vacuum, and radiation stresses in various environments.
- The light sources must be capable of delivering sufficient optical power to the cross-point photodetectors.
- Dynamic range of the photodetectors must be large enough to allow different power levels at the crosspoints.

4.4 CAPABILITY OF OPTOELECTRONIC SWITCHING

The capability of optoelectronic switching depends on the switching architectures and the characteristics of the photodetectors in a switch matrix. The capability is measured by switching speed, isolation, crosstalk, insertion loss, total power dissipation, and switch matrix size. Each of these parameters is discussed as follows:

A. Switching Speed

The switching speed of today's optoelectronic switching techniques ranges from 100 ns in homojunction p-i-n photodiode to around 20 ps in GaAs photoconductors [29-41]. Table 4 shows the switching speed for various optoelectronic switching devices. Most of the devices listed in Table 4 have a switching speed faster than that required for an SS-TDMA system (10 ns).

B. Switch Matrix Size

The state-of-the-art optoelectronic switch matrix size is 4x8 [42]. This switch matrix size is too small for an SS-TDMA IF switch. With the rapid progress in optical/optoelectronic technology [43], we would expect that monolithic implementation of a 16x16 or 20x20 optoelectronic switch matrix should be possible within the next two years.

Table 4. Switching Speed of Various Optoelectronic Switching Devices.

Device	Switching Speed	References
Homojunction PIN Photodiode	100 ns	29
Heterojunction PIN Photodiode	30 ns	44
Avalanche Photodiode	3 ns	32
GaAs MESFET	100 ps	34
InP Photoconductor	200 ps	39
AlInAs Photoconductor	20 ps	36

C. Isolation

High isolation is one of the advantages that optoelectronic switching offers. Cross-point isolation of more than 80 dB at signal frequencies up to 1 GHz and over 50 dB up to 4 GHz has been demonstrated [44-46]. This will satisfy the 40 dB isolation requirement for an SS-TDMA system.

D. Crosstalk

Low crosstalk is another advantage of optoelectronic switching. Crosstalk of less than -80 dB at multi-gigahertz frequencies are readily attainable in an optoelectronic switch matrix. This low crosstalk is not easy to achieve in an electronic switch matrix, especially at high frequencies.

E. Insertion Loss

Optical losses in optical couplers and waveguides contribute a substantial portion of the total insertion loss of a switch matrix. Only low-loss optical couplers and waveguides are to be used for large switch matrices. To compensate the insertion loss, high respon-

sivity photodetectors and electronic amplifiers may be used at the crosspoints and at the output lines, respectively.

F. Total Power Dissipation

In general, the power dissipation in an optoelectronic switch matrix is comparable to that in an electronic switch matrix of the same size. It depends on the types of optoelectronic elements used in a switch matrix. For example, the power dissipation of an optoelectronic switch matrix using photoconductors as the switching elements is substantially smaller than that of a switch matrix using other types of switching elements.

4.5 OPTOELECTRONIC SWITCHING ARCHITECTURES

In this section we will discuss four optoelectronic switching architectures:

A. Power-divided Switching Architecture

The power-divided switching architecture (Fig. 6) employs optical-power dividers to equally distribute optical power to the crosspoint photodetectors. The switching function is accomplished at the crosspoint photodetectors.

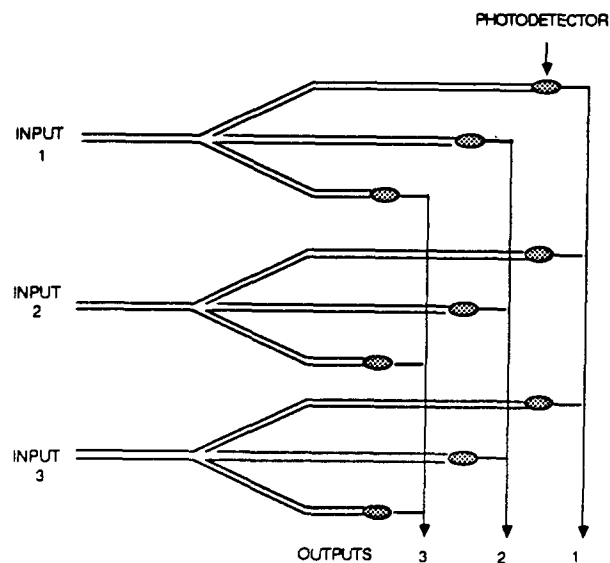


Fig. 6. Power-divided switch architecture.

The optical-power dividers could be either star fiber couplers or guided-wave optical dividers. Using today's technology, twisting and fusing a hundred multi-mode fibers together to form a star coupler is very common. Performance of some typical star couplers are listed in Table 5. The excess loss and port-to-port loss of a coupler increase as the number of ports in a coupler increases. In general, port-to-port losses of these optical dividers are small and their uniformities are good. For example, for a fused-junction optical divider with 8 ports, the insertion loss and uniformity are 0.8 dB and 0.3 dB, respectively [42]. This uniformity in power distribution allows this switching architecture to use small-dynamic-range photodetectors.

Table 5. Performance of typical fiber couplers.

TYPE	PORT TO PORT MAXIMUM LOSS (dB)	EXCESS LOSS
4X4	8	36.61%
8X8	11.5	43.37%
16X16	16	59.81%
32X32	19	59.72%
64X64	23	68.93%

This architecture can be implemented by using discrete devices, hybrid integration, or monolithic integration and is a good candidate for SS-TDMA IF switch.

The major advantages of this architecture are:

- No EMI within the switch matrix.
- Failure of a port results in the loss of only one crosspoint.

B. Crossbar Switching Architecture

The crossbar switching architecture (Fig. 7) is similar to the power-divided switching architecture in structure. The differences are that, in this architecture, there are many optical power-dividers along the paths and the optical power is not equally divided at any point. This switching architecture has all the advantages offered by the power-divided switching architecture. In addition, this switching architecture can easily be constructed in a modular form so that larger matrices can be built using the basic modules. Redundancy can also be embedded in the switch matrix without any difficulty. This architecture is also a potential candidate for SS-TDMA IF switch applications.

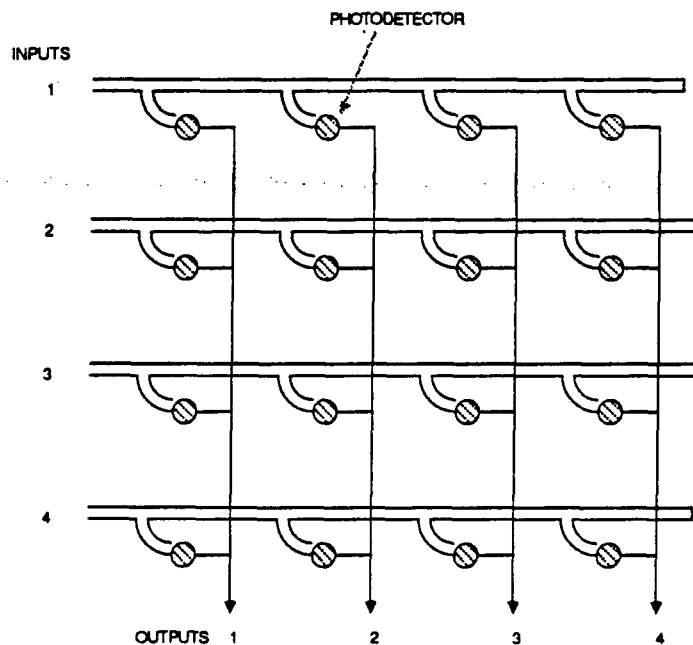


Fig. 7. Crossbar switching architecture.

In this architecture, distribution of optical power to the photodetectors can be accomplished by using either T type fiber couplers or integrated optical waveguides. In a T type fiber coupler, an incoming optical signal is split into two signals. The splitting ratio (power ratio of the two signals) is pre-made and is determined by the structure of the fiber couplers. No external control is needed for the splitting. When fiber couplers are used, it can be shown that the maximum number (N) of fiber couplers that can be cascaded along an optical power distribution path is given by

$$N = \log(r/pc)/\log(1-\alpha-c), \quad (1)$$

where r is the sensitivity of the photodetectors, p is the laser power, and α and c are the excess loss and coupling coefficient of the fiber couplers, respectively. Figure. 8 plots N versus α for various laser power levels. Note that the excess loss of the fiber couplers plays a very important role in determining the number of fiber couplers that can be allowed along an optical power distribution path. A plot of N versus laser power is shown in Fig. 9. As can be seen from this figure, a large increase in laser power does not help much in making N much larger. A similar conclusion may be drawn if we attempt to increase the sensitivity of the photodetectors. Therefore, the most efficient way to make a large switch matrix is to reduce the excess loss of the fiber couplers. This can avoid the excess power requirement in the laser diodes and the high sensitivity requirement in the photodetectors.

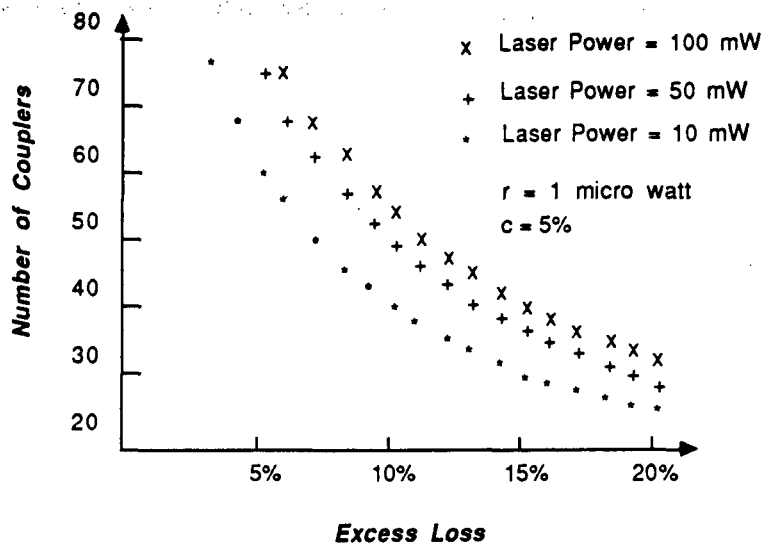


Fig. 8. Maximum number of fibers per line versus excess loss.

Along an optical power distribution path, the optical power delivered to the photodetectors may range from milliwatts at the first crosspoint to microwatts at the last crosspoint. Thus, the photodetectors must have a dynamic range of 30 dB. To alleviate this large-dynamic-range requirement, the optical power distribution system may be designed

in such a way that the optical power delivered to the photodetectors increases from a small percentage at the first crosspoint to a large percentage at the last crosspoint. For example, if there are N crosspoints along an optical distribution path, $1/N$ of the optical power will be distributed to the first crosspoint photodetector and $1/(N-n+1)$ of the remaining optical power will be distributed to the n -th crosspoint photodetector, where n is an integer smaller than or equal to N .

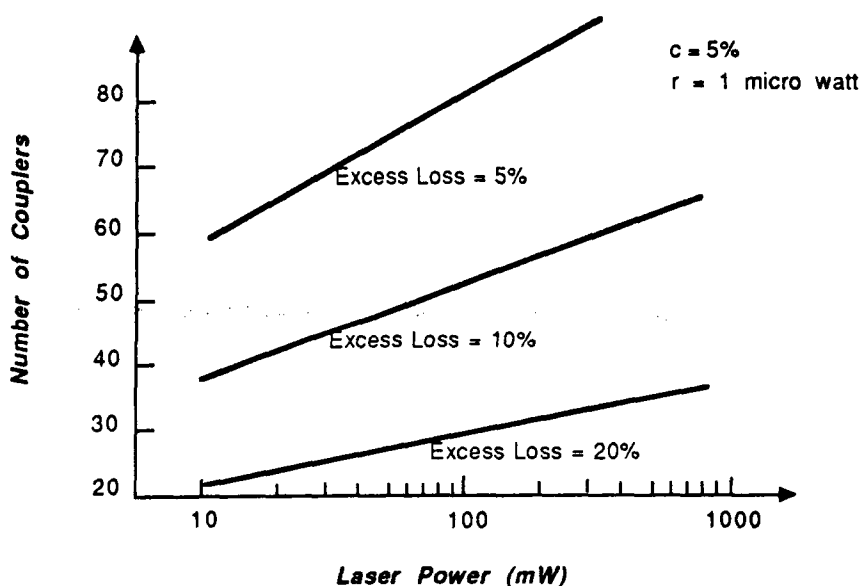


Fig. 9. Maximum number of fibers per line versus laser power.

For one-to-one switching, direction of optical power to the crosspoints may also be accomplished by using LiNbO_3 -based directional couplers or cross couplers (Fig. 10). In these couplers, the optical power is directed to either output port of the coupler by controlling the voltages applied to the electrodes. These couplers are referred to as active optical couplers. In the switching architecture shown in Fig. 10, switching functions are accomplished at the couplers; the photodetectors serve purely as photoreceivers and are always biased at "ON" state. Use of active optical couplers for one-to-one switching may be more advantageous for small switch matrices from the power budget viewpoint. However, from the control point of view, using passive fiber couplers is simpler than using active optical

couplers. Moreover, power loss in a large switch matrix using discrete active optical couplers could be extremely high because of the unavoidable coupling loss at the input and output ends of the couplers. Figure 11 shows a comparison of the power level received by individual photodetectors for a switch matrix using active optical couplers and using passive fiber couplers. From this figure we can see that for small switch matrices, the received power levels are higher by using active optical couplers than by using passive fiber couplers. But, for large switch matrices, the use of active optical couplers results in lower received power levels.

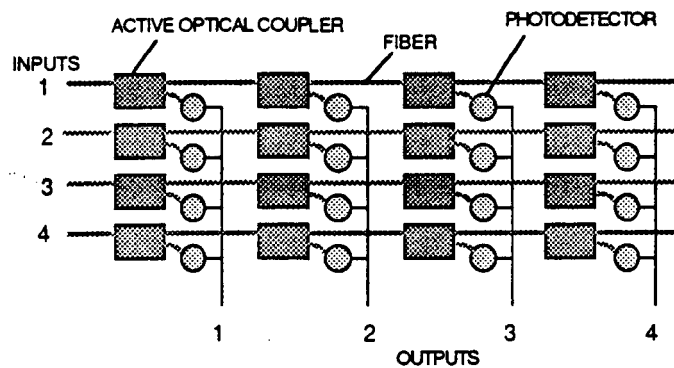


Fig. 10. A crossbar switching architecture using active optical couplers.

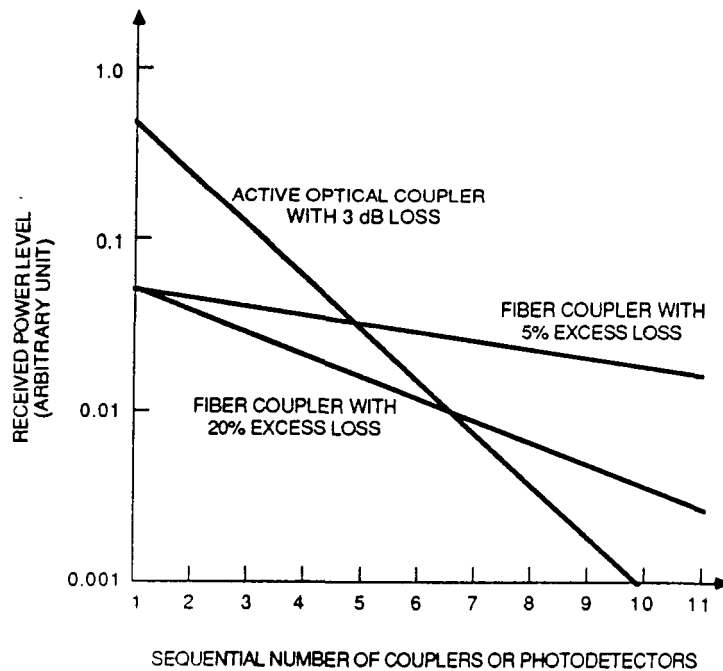


Fig. 11. Comparison of received power levels at photodetectors.

C. Optical-coupled Switching Architecture

The optical-coupled switching architecture operates in quite a different way from that of the optical-divided switching architecture. As shown in Fig. 12, this architecture utilizes an array of optical couplers to switch the light into one path or the other. The switching function is accomplished by changing the voltages of the couplers. The photodetectors are always maintained at their "ON" state.

Many types of optical couplers can be used in this switch architecture. These include waveguide crossover couplers [47], directional couplers [48,49], and balanced bridge interferometer switches [50,51]. All of these optical couplers operate through a voltage-induced change in the refractive index of the waveguide.

The advantages of this architecture are its mechanical stability and immunity to environment perturbations. However, this architecture cannot perform one-to-many and broadcast modes of switching. High insertion loss and temperature instability of the optical couplers may also prevent this architecture from being applied to IF switch matrices.

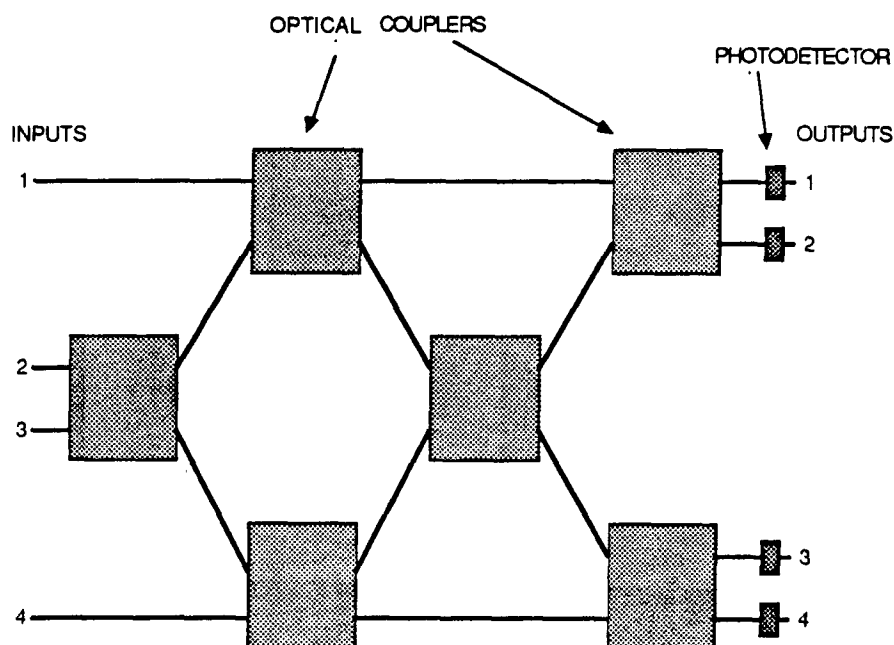


Fig. 12. Optical-coupled switching architecture.

D. Holographic Switching Architecture

The holographic switching architecture is essentially a three dimensional space switch using diffraction principle. It is totally different from the above three architectures.

A schematic diagram representing a holographic switching architecture is shown in Fig. 13. The switch consists of two matrices, each containing an array of holograms. The incoming parallel optical beams enter the switch from the left. They are deflected by first hologram array to the designated directions. When the deflected beams reach the second hologram array, they are deflected again to form the parallel outgoing beams, which are then collected by a photodetector array. The switching function is accomplished by controlling the hologram parameters, such as grating directions, spacings, etc. Recently, transient holograms producing large deflection ($> 28^\circ$) and high diffraction efficiency ($> 98\%$) have been demonstrated using a photorefractive material [52,53]. These transient holograms could be employed in the holographic switching architecture.

The major advantages of the holographic switching architecture are: (1) small insertion loss because of high diffraction efficiency of the holograms and (2) bandwidth independency of the switch. However, the switching speed is slow (approximately $1\ \mu\text{s}$) and control of the holograms needs other light sources or electro-optic devices. In addition, this architecture cannot perform broadcast mode of switching. It is very difficult at present or within the next two years to use this architecture in IF switches.

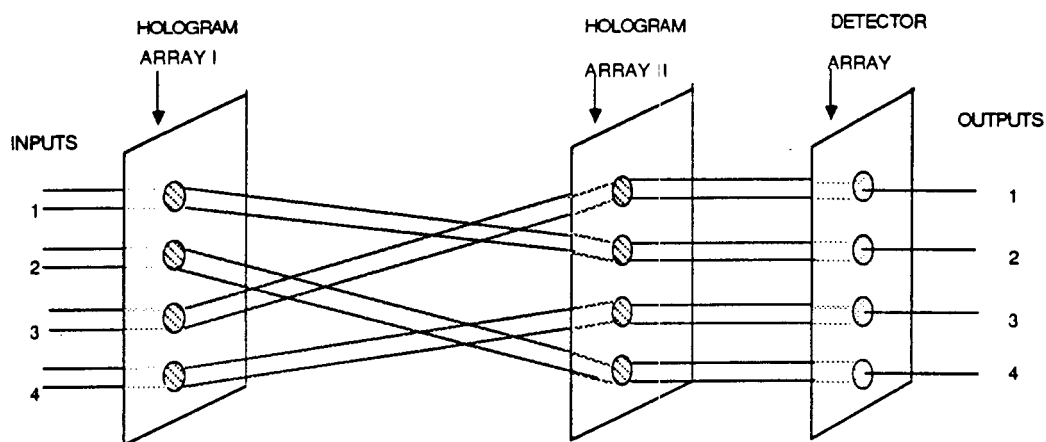


Fig. 13. Holographic switching architecture.

D. Holographic Switching Architecture

The holographic switching architecture is essentially a three dimensional space switch using diffraction principle. It is totally different from the above three architectures.

A schematic diagram representing a holographic switching architecture is shown in Fig. 13. The switch consists of two matrices, each containing an array of holograms. The incoming parallel optical beams enter the switch from the left. They are deflected by first hologram array to the designated directions. When the deflected beams reach the second hologram array, they are deflected again to form the parallel outgoing beams, which are then collected by a photodetector array. The switching function is accomplished by controlling the hologram parameters, such as grating directions, spacings, etc. Recently, transient holograms producing large deflection ($> 28^\circ$) and high diffraction efficiency ($> 98\%$) have been demonstrated using a photorefractive material [52,53]. These transient holograms could be employed in the holographic switching architecture.

The major advantages of the holographic switching architecture are: (1) small insertion loss because of high diffraction efficiency of the holograms and (2) bandwidth independency of the switch. However, the switching speed is slow (approximately $1\ \mu\text{s}$) and control of the holograms needs other light sources or electro-optic devices. In addition, this architecture cannot perform broadcast mode of switching. It is very difficult at present or within the next two years to use this architecture in IF switches.

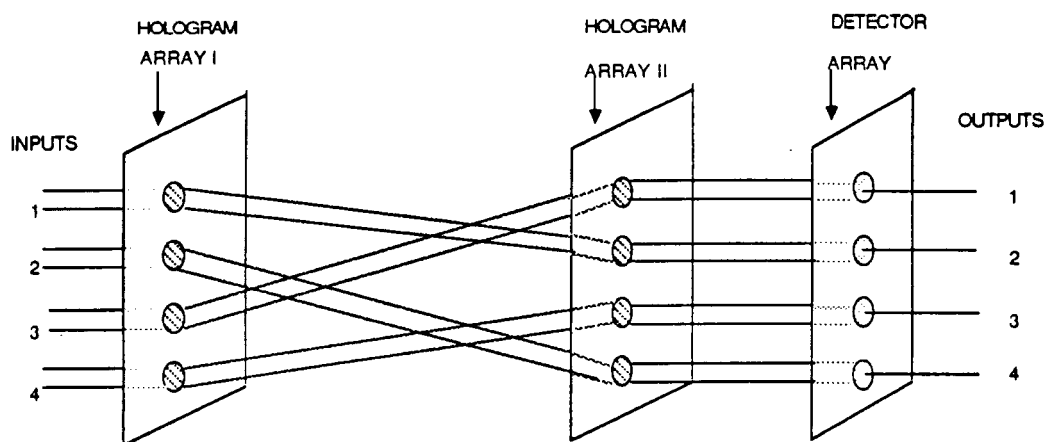


Fig. 13. Holographic switching architecture.

4.6 FEASIBILITY OF EMPLOYING OPTOELECTRONIC SWITCHING ARCHITECTURES IN AN IF SWITCH

Exploration of various switching architectures revealed that both the power-divided and the crossbar switch matrices are possible candidates for SS-TDMA IF switches. A comparison of these two architectures is summarized in Table 6. The technologies required for these architectures, such as tapered-fiber technology, diode laser technology, and photodetector technology, already exist. The major improvement required is the integration technology that is capable of integrating light sources, optical distribution elements, and photodetectors into a small and compact switch matrix containing many input and output lines. This will rely on the progress in integrated optoelectronics. With current integration technology, relatively small optoelectronic switch matrices can be built. In view of the rapid progress in integrated optoelectronics [43], we believe that large-scale monolithic integrated optoelectronic switching circuits can be realized in the near future. Employment of optoelectronic switching techniques in IF switches seems very feasible.

Table 6. Comparison of the crossbar and power-divided switching architectures.

	CROSSBAR ARCHITECTURE	POWER-DIVIDED ARCHITECTURE
COUPLERS USED	PASSIVE FIBER COUPLERS ACTIVE OPTICAL COUPLERS	PASSIVE FIBER COUPLERS
MODULARITY	NON EXPANDABLE (BASIC MODULE) EXPANDABLE (SWITCH MATRIX)	NONEXPANDABLE (BASIC MODULE) EXPANDABLE (SWITCH MATRIX)
PORT TO PORT LOSS	HIGH	LOW

4.7 MODULARITY OF THE CANDIDATE SWITCHING ARCHITECTURES

As shown in Fig. 7, the crossbar switch matrix consists of a set of optical power distribution lines. Each line has a light source at its input and one photodetector at each of its

crosspoints. Each line (Fig. 14a) can be considered as a basic module. A switch matrix, large or small, can be constructed by using this basic module as a building block. For example, a 20x20 switch matrix can be constructed by using 20 lines (basic modules). The matrix size can be expanded by adding more lines to the original switch matrix without reconstruction. However, in an on-board satellite environment, it will be more practical and economical to construct a larger-than-required switch matrix to provide for future expansion. For example, a 80x80 switch matrix could be built for serving 20 uplinks and 20 downlinks. Only 20 lines in the switch matrix are being used. The other 60 lines could be used for redundancy and expansion purposes.

The basic module in the power-divided switching architecture is shown in Fig. 14b. It consists of a light source, a multi-port (star) fiber coupler, and the crosspoint photodetectors. This module has a smaller insertion loss than the basic module in crossbar switching architecture because of the uniform power distribution among the crosspoints.

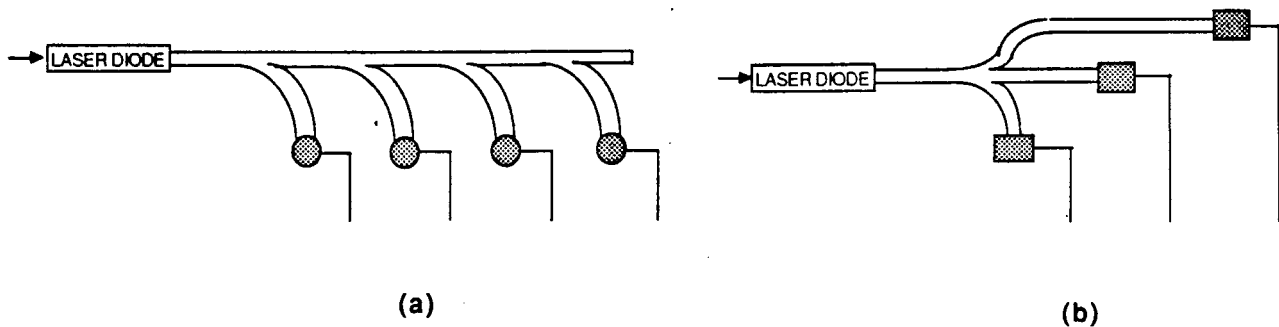


Fig. 14. Basic modules for (a) crossbar and (b) power-divided architectures.

Chapter 5

SYSTEM COMPONENTS

In this chapter, we will describe the system components: optical sources, couplers, and photodetectors.

5.1 OPTICAL SOURCES

The technologies of light emitting diodes (LEDs) and semiconductor lasers have matured to a point where many of these devices have already been deployed in communication systems. Currently, a variety of LEDs and laser diodes are available to cover the wavelength region from 0.8 to 1.6 μm . Although LEDs and laser diodes can equally be used in many applications, laser diodes seem to be the better choice for applications in optoelectronic switching because they allow high modulation rates (on the order of Gb/s) and deliver high optical power. Therefore, only laser diodes will be discussed in this section.

5.1.1 *Basic Operation and Device Structures of a Laser Diode*

The light emitted by a laser diode comes from the recombination of electrons and holes at a p-n junction as an injection current flows through the diode under forward bias. An electron from the n-layer conduction band recombines with a hole from the p-layer valence band, emitting a photon.

A basic laser diode (Fig. 15) consists of two cleaved parallel facets and two roughened sides. The two cleaved facets form a Fabry-Perot cavity. The active region of the laser is a thin planar waveguide, in which the electron-hole recombination occurs. The radiation is also confined and amplified inside the the waveguide. The original laser diodes were homojunctions.

Recently, with a goal of trying to reach single mode operation with minimal threshold currents, many different device structures have been developed. These include single heterojunction, double heterojunction, quadruple heterojunction, large optical cavity, distributed feedback, distributed Bragg reflection, and cleaved-coupled-cavity structures. We

will not attempt to discuss these device structures in detail but will briefly describe their key features.

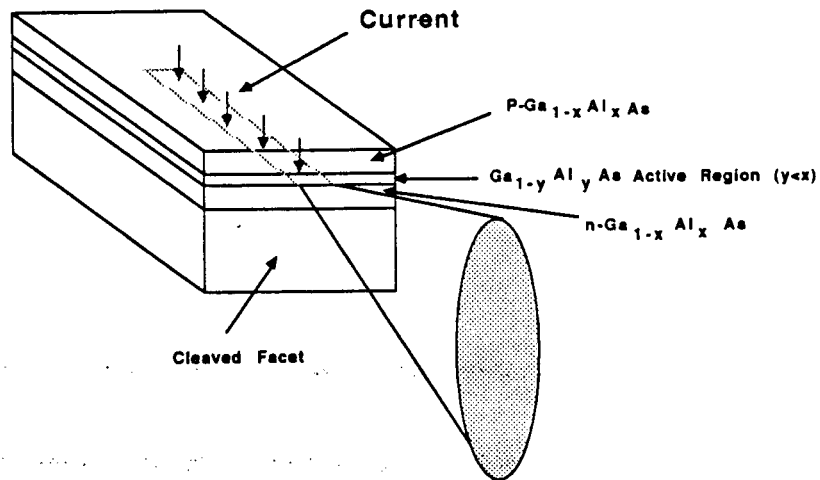


Fig. 15. Laser diode structure.

- Homojunction structure: The recombination region width is set by minority carrier diffusion length. The radiation confinement is the result of refractive index gradients and carrier concentration differences.
- Single heterojunction structure: The heterojunction forms a potential barrier for carrier confinement within the recombination region, as well as one boundary of the waveguide. Asymmetrical waveguide is formed within the refractive index step at the heterojunction.
- Double heterojunction structure: The recombination region is bounded by two higher bandgap regions to confine the carriers and the radiation. The device can be made symmetrical or asymmetrical. The two heterojunctions can be fabricated very close to each other so that the recombination region is extremely thin but still provide full confinement. This can minimize the divergence while keeping the desirable current density for room temperature CW operation.

- **Quadruple heterojunction structure:** This is an extension of the double heterojunction structure. The recombination region is generally centered within the waveguide region. By adjusting the refractive index step between the recombination region and adjoining regions, the fraction of radiation within the recombination width and the interaction with the two outer heterojunctions can be adjusted. This structure allows the maximum design flexibility.
- **Large optical cavity structure:** This structure has a wider waveguide region than the recombination region, which occupies one side of the space between the two major heterojunctions. This device structure was intended for efficient pulsed power operation.
- **Distributed feedback structure:** The active region waveguide is a periodic structure which forms a distributed reflector that turns the waveguide itself into a wavelength-sensitive resonator. The purpose of this structure is to reduce the number of longitudinal modes.
- **Distributed Bragg reflection structure:** The distributed reflector is formed on a waveguide region separate from but coupled to the active region. This structure can also reduce the number of longitudinal modes.
- **Cleaved-coupled-cavity structure:** This laser consists of two Fabry-Perot cavities coupled by a small air gap. Only those wavelengths that are common to both cavities are allowed, so that the output is of high spectral purity. By adjusting the injection currents in the two lasers, one can shift the output wavelength in steps over a wide range (approximately 10 nm).

5.1.2 ***Advantages and Disadvantages of Laser Diodes***

Laser diodes have many advantages over LEDs. The major advantages are:

- **Narrow emission spectra ($< 2 \text{ nm}$).**

- Wide modulation bandwidth (> 2 GHz).
- Efficient coupling into fibers (about 50%).


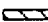
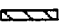








There are also some disadvantages of laser diodes. Typical ones are:

- More critical construction is needed for high performance, affecting present cost.
- Threshold current may double when temperature changes from 20 to 70 °C, requiring temperature stabilization or optical feedback to control output.
- Linearity of power versus current depends on operating conditions - linear region above threshold only.

5.1.3 Material and Output Characteristics of Laser Diodes

From the material point of view, typical laser diodes are normally categorized into two groups: AlGaAs devices on GaAs for wavelengths between 0.8 and 0.9 μm and InGaAsP devices on InP for wavelengths between 1.3 and 1.6 μm . Other materials such as II-VI and IV-VI compounds have also been used for laser diodes emitting visible and far-infrared light. Some important laser diode materials are summarized in Table 7.

Table 7. Materials for semiconductor light sources.

Material			Emission Wavelength (micron)
Active	Cladding	Substrate	
III-V			0.5 1.0 5 10
AlGaAs	AlGaAs	GaAs	
GaInAsP	GaInP	GaAs	
GaInAsP	GaInP	GaAs	
GaInAsP	AlGaInP	GaAs	
AlGaInP	AlGaInP	GaAs	
GaInAsP	AlGaAs	GaAs	
GaInAsP	InP	InP	
AlGaAsSb	AlGaAsSb	GaSb	
InAsSbP	InAsSbP	InAs	
IV-VI			
PbSnSeTe	PbSnSeTe	PbTe	
II-VI			
ZnSSe		GaAs	

The output optical power of a laser diode is limited by the ability of the active region to dissipate the heat generated by nonradiative processes as well as by its internal resistance. It is also limited by the maximum optical power density that the resonator can support. The output characteristics of some typical laser diodes are shown in Table 8. Note that typical device efficiencies (total output optical power divided by total input electrical power) are on the order of 40 to 45%.

Table 8. Output characteristics of diode lasers.

TYPE	WAVELENGTH (microns)	TYPICAL POWER (mW)	MAXIMUM POWER (mW)	QUANTUM EFFICIENCY %	DEVICE EFFICIENCY	T _j °C	T _j MAX °C	I _o mA
GaAlAs/GaAs								
LED	0.85	10	200		45			
LD	0.85	5-10	200	50-70	40	120-150	150 (CW) 276 (pulsed)	4.5
LD Out. Wall	0.85	1.6		80		200		2.5
LD Phs. Ary.	0.85		2600	60				
InGaAsP/InP								
LED	1.3	1						
LD	1.3	5-10	140	50-70	43	50-70	142 (CW)	
LD	1.55	5-10	40	40-60		40-60	115 (CW)	
LD Sig. Mode	1.3	5-10	60	30 (per facet)				
LD Sig. Mode	1.55	5-10	20	20 (per facet)				

REFS: S. Suematsu, Phys. Today, May 1985
D. A. B. Miller, J. Quantum Electron., Sept., 1985

5.1.4 Modulation of Lasers

In an optoelectronic switching architecture, conversion of the incoming electrical signals to optical signals can be accomplished via internal or external modulation. For internal modulation, the laser output is modulated by controlling the injection current of the laser diode. The main advantage of internal modulation is its simplicity. As shown in Fig. 16, with the laser biased above threshold and the incoming electrical signal superimposed on the drive current, the output of the laser is an analog of the incoming electrical waveform. High bandwidth internal modulation can be achieved using InGaAsP lasers. A modulation bandwidth of 15 GHz has been reported for vapor-phase regrown 1.3 μm InGaAsP buried-heterostructure lasers by researchers at GTE Laboratories [54]. Commercial laser

diodes from Hitachi can easily be modulated at 2 GHz. For low temperature (-70°C) operation, a modulation bandwidth of 22 GHz can be achieved [55]. One disadvantage of internal modulation is frequency chirping - laser frequency varies in response to the signal component of the drive current.

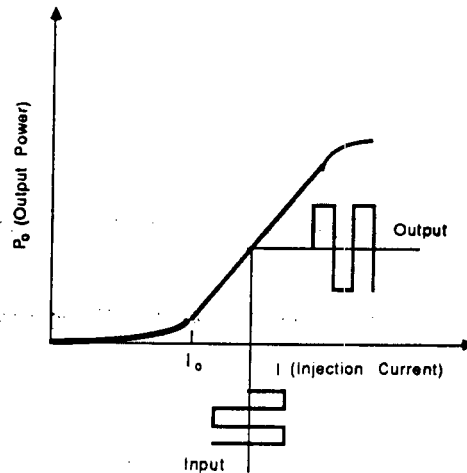


Fig. 16. Internal modulation of a laser diode.

For external modulation, the incoming electrical signal modulates the bias of a modulator and produces a light signal which is a replica of the incoming electrical signal. A typical LiNbO_3 -based Mach-Zehnder interferometric modulator is shown in Fig. 17. The highest modulation bandwidth reported is around 17 GHz [56]. Typical modulation rate ranges from 2 GHz to 10 GHz. For high-speed communication the use of external modulation is an attractive alternative to direct modulation of semiconductor lasers. Using external modulation, frequency chirping is minimized and modal partition noise is reduced. However, one major limitation to the use of a conventional external modulator is its polarization dependence. Incorrect polarization of the input light reduces the modulation depth and consequently degrades the optimum extinction ratio of the modulated light.

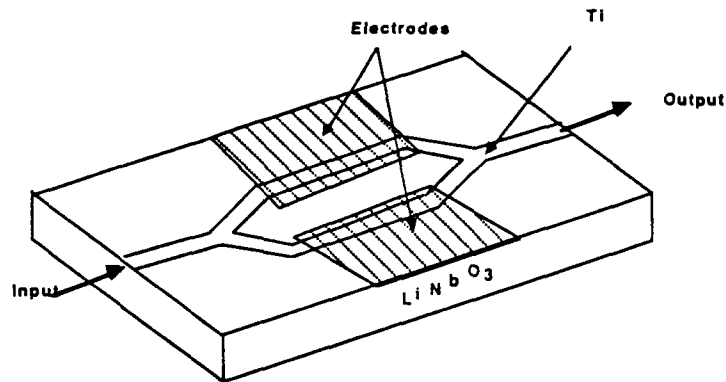


Fig. 17. An external modulator.

5.1.5 Selection of Laser Diodes

From a practical point of view, how to select a suitable laser diode for a specific application is extremely important. Listed below are some of the major issues that should be considered when selecting a laser diode.

1. Compatibility with particular optical fiber to be used
 - a) Wavelength match - to achieve low loss
 - b) Maximum coupling efficiency
 - c) Group delay distortion (spectral width and mode content)
2. Modulation requirements
 - a) Information rates
 - b) Modulation format
 - c) Pulsed or CW output
3. Optical output power
4. Stability of the output power
 - a) Thermal
 - b) Spectral
5. Reliability and lifetime - Device mean-time-before-failure
6. Cost effectiveness

- a) Initial cost
- b) Maintenance
- c) Part replacements

7. Physical requirements

- a) Space
- b) Power
- c) Temperature and humidity

Based on the above considerations and availability of the laser diodes, heterojunction laser diodes seem to be the most suitable optical sources for optoelectronic switching.

5.2 COUPLERS

The basic function of an optical coupler is to distribute information to and from multiple-access environments. Generically, there are two types of couplers: the T and the star couplers. These couplers can be constructed using optical fibers or guided-wave material such as Ti-diffused lithium niobate. The couplers made of optical fibers are called passive fiber couplers because the splitting ratios of the couplers are pre-made and information is distributed to all outputs. Couplers using guided-wave material, such as LiNbO₃-based directional couplers, are called active optical couplers. In an active optical coupler, the information is either directed to one output or the other and there is no splitting ratio involved.

5.2.1 *Passive fiber couplers*

A passive fiber coupler is made by twisting and fusing N optical fibers together. A NxN star coupler is illustrated in Fig. 18 as an example. The excess loss of the coupler is due to its power scattering at the junction of the fibers. The optical power is equally divided among the N fibers. For a T type coupler, the splitting ratio can be 80-20, 95-5, or other combinations as requested by the user. The insertion loss of the coupler is defined as:

$$P = -10 \log(P_o/P_i), \quad (2)$$

where $P_o = (P_i - \text{excess loss at the junction})/N$ and P_i is the input optical power.

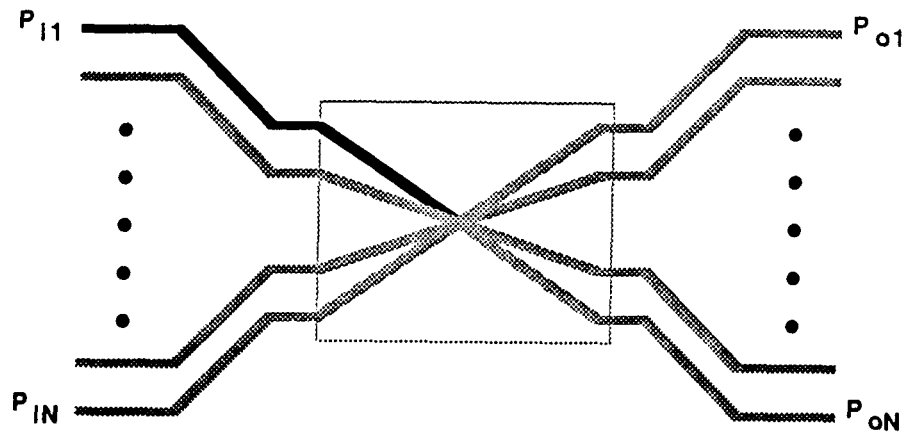


Fig. 18. An NxN star coupler.

5.2.2 Active Optical Couplers

The most widely used active guided-wave couplers for optical communication applications is the Ti:LiNbO₃ directional coupler. Figure 19 shows the generic diagram of the directional coupler. Two channel waveguides of identical refractive index and width are positioned next to each other for a certain distance. Light traveling through one waveguide penetrates slightly into the other, coupling the two waveguides. Complete transfer of light from one waveguide to the other takes a specific length κ . Beyond this distance, light begins to couple back to the original waveguide, and is completely returned at two transfer lengths. The transfer length κ depends on the waveguide parameters, the interwaveguide gap d , and the guided wavelength λ . Light coupling between the two waveguides also depends on the interaction length and on the difference in propagation constants between the two waveguides, $\Delta\beta = (2\pi/\lambda)(n_2 - n_1)$, where n_2 and n_1 are the effective indexes. If the two identical waveguides are adjacent for exactly the length it takes for a complete transfer to occur, then the system acts as a "cross-state" coupler. If they are adjacent for an even number of transfer lengths, the signal returns to the original waveguide, and the coupler is said to be in a "through state". However, this type of coupler is extremely difficult to fabricate because the length for which the two waveguides lie adjacent and their widths along

this distance must be fabricated with absolute precision. The $\Delta\beta$ reversed coupler (Fig. 20) combines the principle of the directional coupler with the electro-optic effect, in which an applied voltage changes the waveguide's refractive index. Using this effect, the transfer length is modified so that one set of voltages on the electrodes puts the coupler in the "cross state", and the other sets it in the "through state".

For a typical 2x2 coupler at $\lambda = 1.3 \mu\text{m}$, the insertion loss is about 3 dB. This insertion loss is mainly due to (i) the waveguide propagation loss, (ii) the input and output coupling losses, and (iii) the reflection losses at LiNbO₃ facets and output fiber facets. The typical dimensions of a directional coupler are 3-9 mm in length and 100-300 μm in width. "Cross state" of this device is about 25 dB with electrode voltages between 5 and 10 volts.

The cross coupler (Fig. 21) is another type of active optical coupler. In this coupler, the two waveguides intersect each other. Selection of "cross state" or "through state" is also accomplished by varying the electrode voltages.

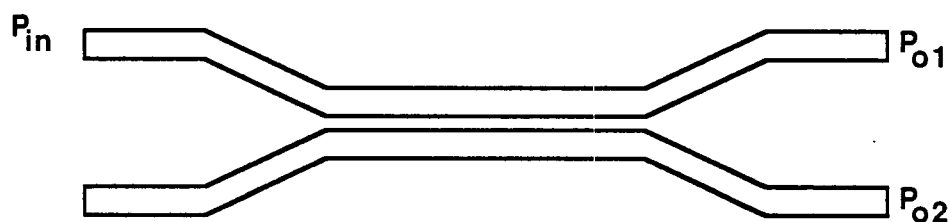


Fig. 19. A generic directional coupler.

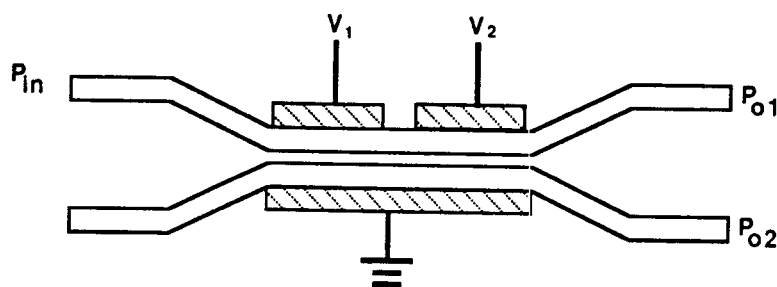


Fig. 20. A $\Delta\beta$ directional coupler.

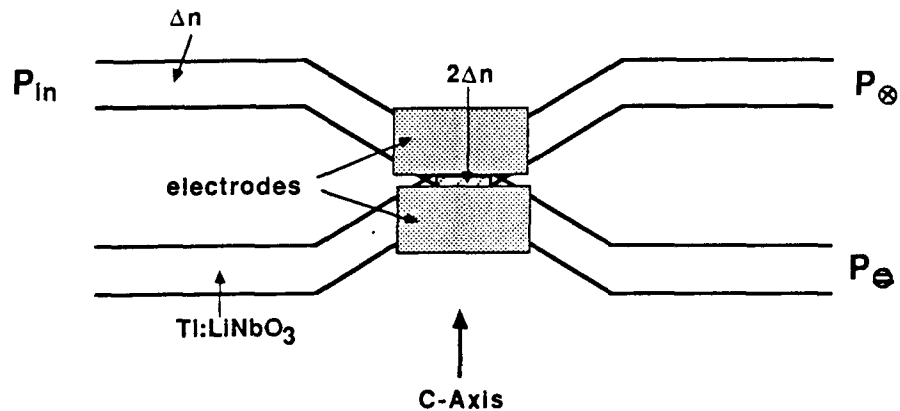


Fig. 21. A cross coupler.

5.3 PHOTODETECTORS

In an optoelectronic switch matrix using passive fiber couplers, photodetectors are the crosspoints to perform switching. PIN photodiodes, avalanche photodiodes, Schottky barrier photodiodes, and photoconductors are the four basic devices that have a frequency response up to tens of GHz. The silicon-based devices can respond to wavelengths up to 1 μm . In the 1 to 1.6 μm region Ge and InGaAs are the candidate materials. In this section, major features of these devices are briefly discussed. Detailed discussions of photodetectors may be found in Refs. 57 - 65.

5.3.1 PIN Photodiodes

A PIN photodiode consists of a large intrinsic region sandwiched between p- and n-doped semiconducting regions (Fig. 22). Photons absorbed in this region create electron-hole pairs that are then separated by an electric field across the region, generating an electric current in the load circuit.

Efficiency of the photon to electron-hole pair conversion process is specified by the photodiode's quantum efficiency, η . The quantum efficiency is a function of wavelength and temperature. Another important parameter in a photodiode is its responsivity. It is re-

lated to the quantum efficiency by $r = \eta \lambda / 1.24$. This is the ratio of the output current to the incident optical power, measured in A/W. Typical responsivity of a silicon PIN diode is about 0.7 A/W at $\lambda = 0.8 \mu\text{m}$.

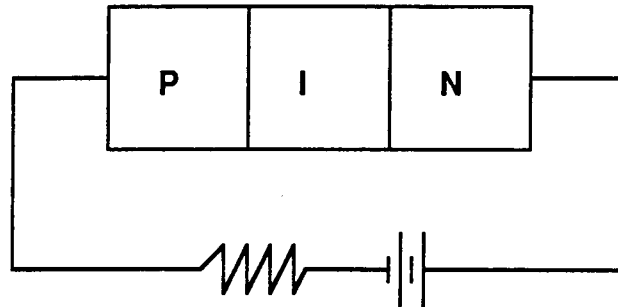


Fig. 22. A PIN photodetector.

When used in an optoelectronic switching matrix, the response speed of the PINs is very important. The speed of PIN photodiodes is limited by (i) the carrier transit time through the depletion and intrinsic regions and (ii) the parasitic capacitances. The transit time is the fundamental limit, but is normally not the limiting factor in a practical application. The dominant effect on the speed performance is the parasitic capacitance. To minimize this capacitance, the diode must be made small. In general, PIN photodiodes have a response time ranging from a few nanoseconds to a few hundred picoseconds.

5.3.2 *Avalanche Photodiodes*

An avalanche photodiode is designed for greater sensitivity. Because of a strong electric field arising within it as a result of external biasing, the APD exhibits an internal gain mechanism. Primary electrons are accelerated and undergo ionizing collisions with surrounding atoms, generating more electrons.

Among a variety of APDs, the separate absorption grading multiplication avalanche photodiode (SAGM APD) is the best-performing photodetector for high bandwidth (or high bit rate) applications. The cross-section structure of a SAGM APD is shown in Fig. 23. Photons in the wavelength region 1.2 to 1.6 μm enter the detector through a number of transparent layers: the InP substrate, the p and n epitaxial InP multiplication layers, and the

InGaAsP grading layer. The relatively thick InGaAs layer absorbs the photons, and the photo-generated electrons/holes drift into the high field region near the p-n junction, where they undergo multiplication.

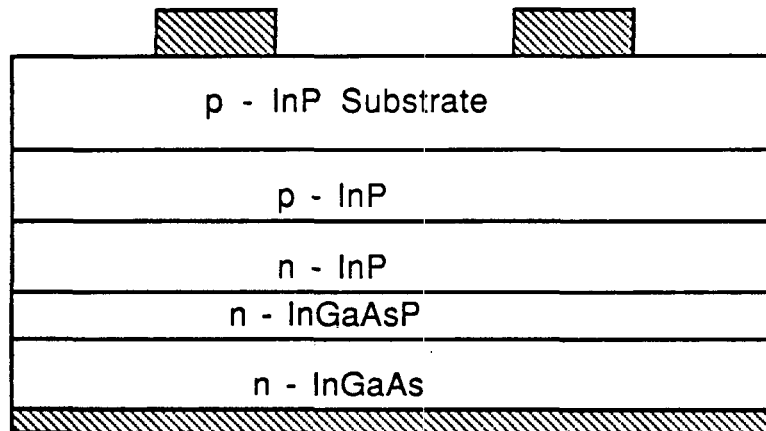


Fig. 23. An SAGM APD.

An APD requires a considerably higher bias voltage than PIN photodiodes. The bias voltage is on the order of 100 to 120 volts. Because of their current gain, APDs can have an order of magnitude higher responsivity than PIN photodiodes. Bandwidth performance of an APD is fairly good. APDs have already achieved a gain-bandwidth product of 60 GHz operating up to 7 GHz [58]. For lower frequency operation, the gain-bandwidth product can go as high as 250 GHz. To reach operation beyond 10 GHz, more work needs to be done on balancing material and structure design to reduce capacitive and resistive effects while providing high absorption efficiency and controlled ionization.

5.3.3 Schottky Barrier Photodiodes

Schottky barrier photodiodes were developed to alleviate the speed limitations encountered in regular photodiodes. Figure 24 shows the cross-section of a GaAs Schottky photodiode. The diode consists of a thin layer of semi-transparent metal film forming the Schottky contact to an n^- -GaAs epitaxial layer grown on an n^+ -GaAs substrate. Recent work on high-speed Schottky barrier photodiodes [60] has shown that their frequency re-

sponse is 100 GHz with an operating reverse bias of 4 volts. The prospect of Schottky barrier photodiodes with a response frequency greater than 100 GHz is very optimistic.

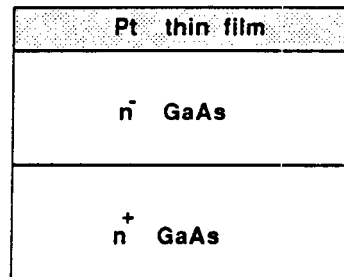


Fig. 24. A Schottky barrier photodiode.

5.3.4 Photoconductors

Photoconductors have been employed in numerous photodetection applications for quite a long time because of their simplicity and their high sensitivity for the detection of weak optical signals. Photoconductors have high switching speeds when used in an optoelectronic switch matrix. This is because a photoconductor does not have a junction in its photosensitive region. A photoconductor is easy to fabricate and can be easily integrated with MESFETs and other planar microwave devices. The materials used for photoconductors are either silicon or III-V materials. However, the silicon-based photoconductors have a relatively low gain-bandwidth product, limiting their usefulness in applications requiring both high sensitivity as well as high switching speeds. Recent studies [61-65] have shown that GaInAs photoconductors are very good candidates for optoelectronic switching because they exhibit high gains (on the order of 10) at high-bit rates (Gb/s) and their gains are relatively insensitive to temperature variations.

The sensitivity of a photoconductor is determined by its geometry, the recombination time, electron mobility, and the refractive index of the material used. During the past few years, a variety of III-V material photoconductors with different structures have been developed. The most common ones are the InGaAs photoconductors. Figure 25 shows a cross-

sectional view of a typical $\text{Ga}_{0.47}\text{In}_{0.53}\text{As}$ photoconductor. It has two sets of interdigitated ohmic contact electrodes made on the surface layer. A top view of the device is shown in Fig. 26. In general, the electrode fingers are 3 - 5 μm wide by 10 - 300 μm long with an interelectrode spacing of 3 - 5 μm . The main purpose of using the interdigitated structure is to increase the photosensitive area without sacrificing the response speed. Typical values of the photoconductor's sensitivity ranges from 0.3 A/W to 0.5 A/W. The response time is about 100 to 200 picoseconds.

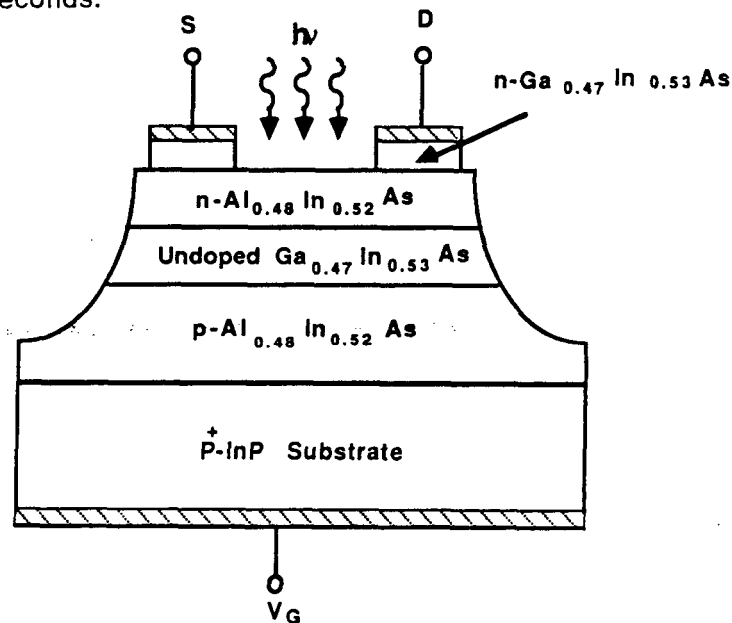


Fig. 25. A photoconductor.

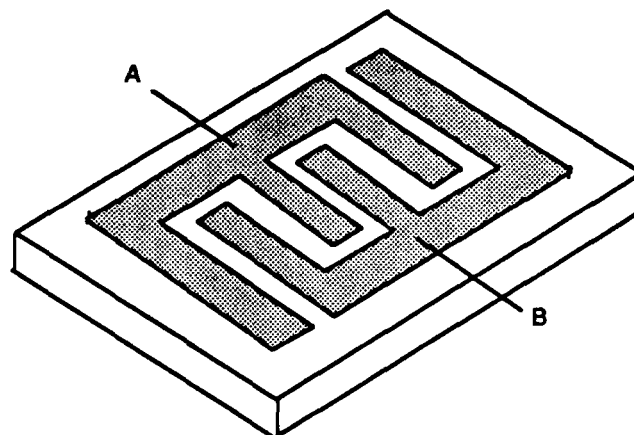


Fig. 26. An interdigitated photoconductor.

Chapter 6

PERFORMANCE EVALUATION OF THE SWITCHING ARCHITECTURES

Performance of an optoelectronic switching architecture can be evaluated by calculating its crosstalk, isolation, insertion loss, matrix size, drive power, throughput, and switching speed.

6.1 CROSSTALK

In an optoelectronic switching architecture, crosstalk exists only among the output electrical lines. Therefore, crosstalk in a switch matrix can be defined as the ratio of the current induced at a neighboring photodetector to the current generated at the primary photodetector. The crosstalk of a switching architecture largely depends on the operation frequency (bit rate), the package parasitic reactances, and the photodetectors. This dependence applies to both crossbar and power-divided switching architectures. Typical measured crosstalks of a switching architecture using different photodetectors and operating at 1.5 GHz are listed in Table 9.

Table 9. Crosstalk between output lines at 1.5 GHz.

PHOTODETECTORS	CROSSTALK
P-I-N DIODE	-30 dB
AVALANCHE PHOTODIODE	-50 dB
PHOTOCONDUCTOR	-50 dB

6.2 ISOLATION

Isolation is independent of the switching architecture. It is solely determined by the operation frequency and the types of photodetectors. Isolation of some photodetectors operating at 1 GHz is shown in Table 10. In general, isolation drops as operation frequency increases. Taking an interdigitated photoconductor as an example, experimental results showed that its isolation of 80 dB at 1 GHz drops to 45 dB at 4 GHz. Also, APDs and photoconductors seem have a better isolation than PIN photodiodes.

Table 10. Isolation of some photodetectors at 1 GHz.

PHOTODETECTORS	ISOLATION
PIN	+50 dB
APD	+80 dB
PHOTOCONDUCTOR	+80 dB

6.3 INSERTION LOSS

Insertion loss of a switch matrix is defined as the ratio of the smallest optical power delivered to a crosspoint photodetector to the input optical power of the corresponding optical distribution line. The insertion loss is determined by the switching architecture, the switch matrix size, and the type of couplers used. For the same matrix size and using the couplers available today, comparison of the crossbar and the power-divided switching architectures showed that the latter has a smaller insertion loss. Based on commercially available couplers, some calculated insertion losses for these two architectures are shown in Table 11. By using commercial couplers, it is not difficult to achieve an insertion loss less than 18 dB for a 20X20 switch matrix. The prospect of constructing switch matrices with matrix sizes larger than 100X100 while keeping the insertion loss under 18 dB looks very good.

Table 11. Calculated insertion loss for some switch matrices.

	Crossbar (2.5%)	Power-divided
4x4	14	8
8x8	15.4	11.5
16x16	18	16
32x32	23.5	19
64x64	34	23

6.4 SWITCH MATRIX SIZE AND THROUGHPUT

The maximum allowable switch matrix size depends on laser power, photodetector sensitivity, coupler excess loss, coupler splitting ratio, and switching architecture. The throughput is a function of switch matrix size and modulation frequency of the lasers. For example, with a laser power of 50 mW and modulation at 4.8 GHz, a minimum detectable power of 1 μ W, a coupler excess loss of 2.5%, and using crossbar switching architecture, the maximum switch matrix size is 100X100 and the maximum throughput is 480 Gb/s.

6.5 POWER DISSIPATION

The power dissipation of a switch matrix is due to (i) the laser driving power and (ii) the power dissipated at the photodetectors. This is also affected by the switch matrix size, excess loss of the couplers, and sensitivity of the photodetectors. For a 20X20 switch, using photodetectors with a minimum detectable power of 2 μ W, the total power needed to drive the 20 laser diodes is about 1.65 W. This was calculated based on the crossbar switching architecture using couplers with an excess loss of 5%. The power dissipated at the photodetectors depends on the type of photodetectors used and the operation mode (one-to-one, one-to-many, and broadcast) of the switch. Our calculations indicate that for a 20X20 switch, power dissipation at the photodetectors is less than 50 W for all modes of operation using photoconductors.

6.6 SWITCHING SPEED

The switching speed of an optoelectronic switch depends on the photodetectors and the switch matrix structure (discrete or integrated). Table 12 shows the switching speeds of a discrete switching matrix using different types of photodetectors. The key to improve the switching speed is to reduce the parasitic capacitances at the photodetectors and in the electronic circuitry. This means that hybrid and/or monolithic integration of the switch matrix is most desirable.

Table 12. Switching speed of optoelectronic devices.

DEVICE	SWITCHING SPEED
HOMOJUNCTION PIN PHOTODIODE	100 nsec
HETEROJUNCTION PIN PHOTODIODE	30 nsec
AVALANCHE PHOTODIODE	3 nsec
GaAs MESFET	100 psec
InP PHOTOCONDUCTOR	200 psec
GaInAs PHOTOCONDUCTOR	20 nsec

Chapter 7

SWITCH MODELS AND OPTIMIZATION

Based on the crossbar and power-divided switching architectures, three models using discrete components, hybrid integration, and monolithic integration will be presented in this chapter. Optimization of these switch models will also be discussed.

7.1 DISCRETE COMPONENT SWITCH MODEL

The discrete component switch model (Fig. 27) consists of discrete AlGaAs/GaAs lasers at the input end, fiber star couplers, and discrete GaAs FETs (used as photoconductors) at the crosspoints. AlGaAs/GaAs ($0.85\text{ }\mu\text{m}$) lasers were selected because of their high reliability, long life time, and low cost. This type of laser can operate at a few gigahertz (limited by electronic circuitry). The fiber star couplers are commercially available (up to four ports for single mode fibers and 64 ports for multimode fibers). GaAs FETs, which are also commercially available, can be used as photoconductors by exposing their gate areas to the optical signals.

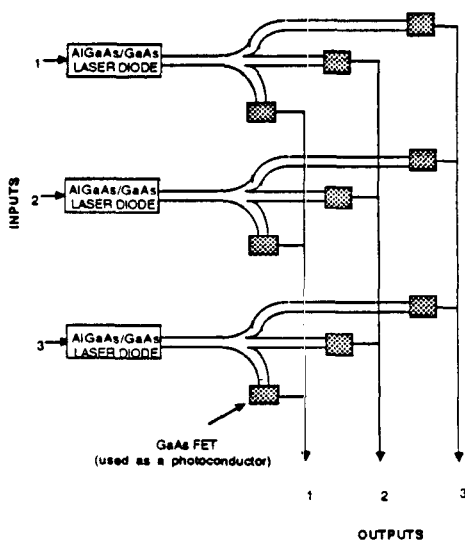


Fig. 27. A 3x3 discrete component optoelectronic switch model.

This switch model is good for demonstrating the concept of optoelectronic switching at reasonable cost. However, because of long electrical wiring among the crosspoints and between the switch elements and the supporting circuitry, this model will have relatively high crosstalk even at low frequencies. To alleviate these problems and improve the performance of this switch model, wire interconnections must be kept short.

Because of its inherent poor performance, this switch model is not recommended for IF switch matrices.

7.2 HYBRID INTEGRATION SWITCH MODEL

The hybrid integration switch model is shown in Fig. 28. A laser diode array is used at the input end. Photoconductor arrays are used for the crosspoints. Distribution of the optical signals is accomplished by fiber couplers.

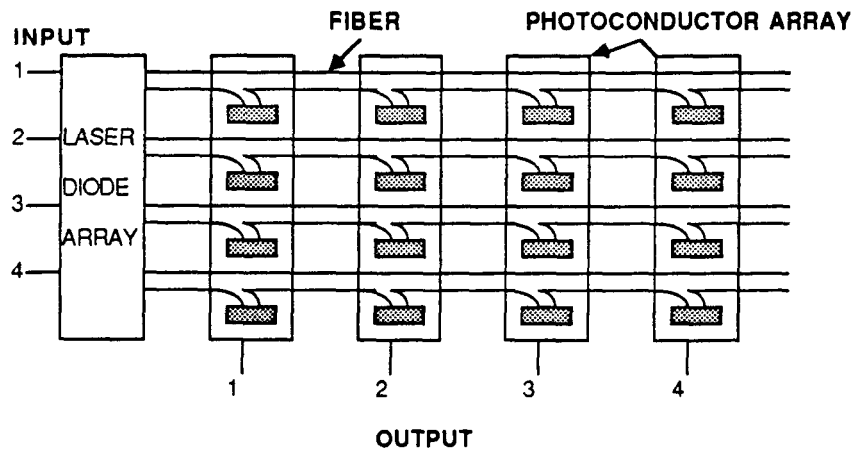


Fig. 28. A 4x4 hybrid optoelectronic switch model.

The laser diode array consists of AlGaAs/GaAs lasers integrated on a substrate. The separations between adjacent lasers are on the order of a few hundred micrometers. The drive circuit can also be integrated on the same substrate, eliminating long interconnections between the lasers and the drive circuits. As a result of this laser/driver integration, the operation frequency can be substantially increased (10 GHz is very typical).

The photoconductor array can be fabricated using a GaAs substrate with interdigitated electrodes deposited on its surface (Fig. 29). The interdigitated areas, which detect the optical signals, have fingers a few micrometers in width and length. The separations between the fingers are also a few micrometers. The structure of the photoconductor array plays an important role in determining the speed and gain of the photoconductor switch elements. Wider separations between the fingers result in higher gain and lower switching speed. Narrowing the separations will increase the switching speed but will reduce the gain. Based on the system requirements, a tradeoff between gain and switching speed must be made in designing a photoconductor array.

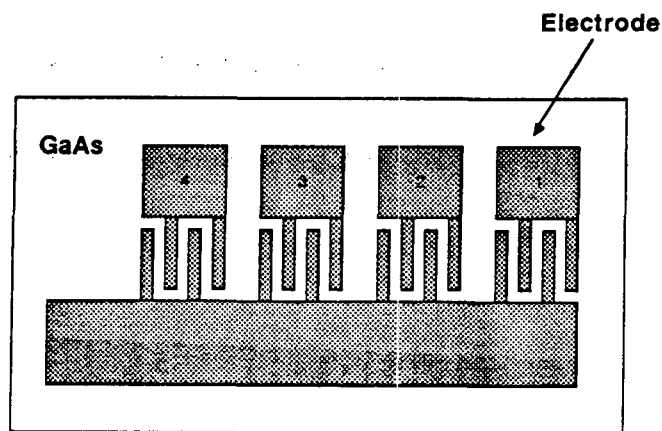


Fig. 29. A photoconductor array.

Performance of the hybrid integrated switch model is better than the discrete component switch model. A switching speed of less than 100 ps is expected because of the integration of lasers, drive circuit, and photoconductor arrays. This model is a good candidate for IF switch matrices. Using today's technology, a 20x20 switch matrix using this model can be built at moderate cost.

7.3 MONOLITHIC INTEGRATION SWITCH MODEL

The ultimate switch matrix is the monolithic integration switch model (Fig. 30). This model offers low interconnect parasitics, a small physical size, and a low power consumption. All of these features are very important for an IF switch matrix. In addition, high

switching speed, high throughput, low crosstalk, and high isolation requirements are also driving the switch matrix toward monolithic integration. Recent progress in optoelectronic integrated circuit (OEIC) technology has made OEIC structures even more possible.

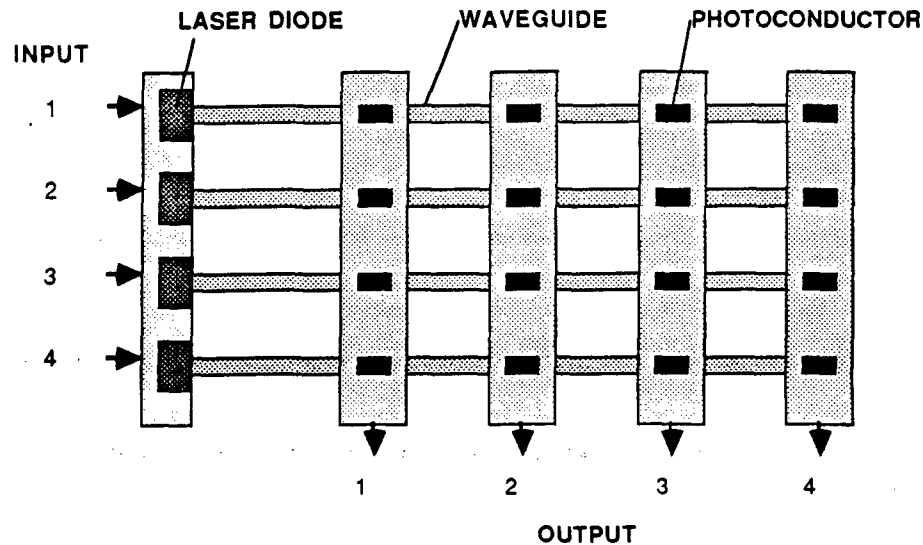


Fig. 30. A 4x4 monolithic optoelectronic switch model.

Compared with hybrid integration, monolithic integration has the following advantages:

- Improved speed and noise performance due to reduction of parasitic reactance.
- Multifunctional capability: light emitting, optical signal distribution, and optical signal detection are integrated within a chip.
- Reduction of the number of components due to dual functions of the integrated devices.
- More compact and reliable.

7.4 OPTIMIZATION OF THE SWITCH MODELS

To optimize a switch model is to minimize the insertion loss and crosstalk and maximize the isolation and switch matrix size. For discrete component and hybrid integration switch models, which use fiber couplers for distributing the optical signals, the most important parameter in determining the switch matrix size and insertion loss is the excess loss of the fiber couplers. How to reduce the excess loss of the fiber couplers is the key to maximizing the switch matrix size and minimizing the insertion loss.

For the monolithic integration switch model, the switch matrix size and insertion loss are determined by integration structure. The crucial factors in monolithic integration are structure planarity, material compatibility, and power dissipation compatibility. Optimization of the monolithic integration switch model depends heavily on the integration technology. Small scale (4x4) monolithic switch matrices can be fabricated with today's technology. However, large scale OEIC fabrication (i.e. 20x20 switch matrix) has not yet been demonstrated.

Crosstalk and isolation are dependent on the electric shielding between output lines and the noise levels (dark currents) of the photoconductors. In the cases of discrete component and hybrid integration switch models, shielding between the output lines can easily be done. For the monolithic integration switch model, a special isolation technique is needed for the photoconductor array. The noise levels of the photoconductors can be reduced by modification of material properties.

Chapter 8

ADVANTAGES AND DISADVANTAGES OF OPTOELECTRONIC SWITCHING SYSTEMS

The major advantages of optoelectronic switching systems are their small size, light weight, low power consumption, and high performance. A hybrid or monolithic integration is necessary to fully exploit these advantages.

8.1 COMPARISON OF MONOLITHIC OPTOELECTRONIC AND GAAS MMIC SWITCHES

Compared with GaAs MMIC, the optoelectronic switching systems have the following advantages:

- Low crosstalk
- High isolation
- Low power dissipation

More specifically, a comparison of some performance parameters of GaAs MMIC and monolithic optoelectronic switch matrices of equal size is listed in Table 13.

Table 13. Comparison of GaAs MMIC and optoelectronic switch matrices.

	GaAs MMIC	OPTOELECTRONIC
Matrix Size	4x4	4x4
Crosstalk (@ 1 GHz)	-28 dB	-80 dB
Isolation (@ 4 GHz)	57 dB	70 dB
Power Dissipation	1.1 W	0.5 W
Operation Voltage	5V	5V

The major drawback of GaAs MMIC is that its crosstalk exists not only among output lines but also among input lines and between input and output lines. As a result, its crosstalk increases not only with operation frequency but also with switch matrix size. Figure 31 shows a simulation result of crosstalk characteristics versus port number. It indicates that when the switch matrix size is larger than 8x8, the crosstalk will be larger than -20 dB. High crosstalks will limit GaAs MMIC to small switch matrix sizes.

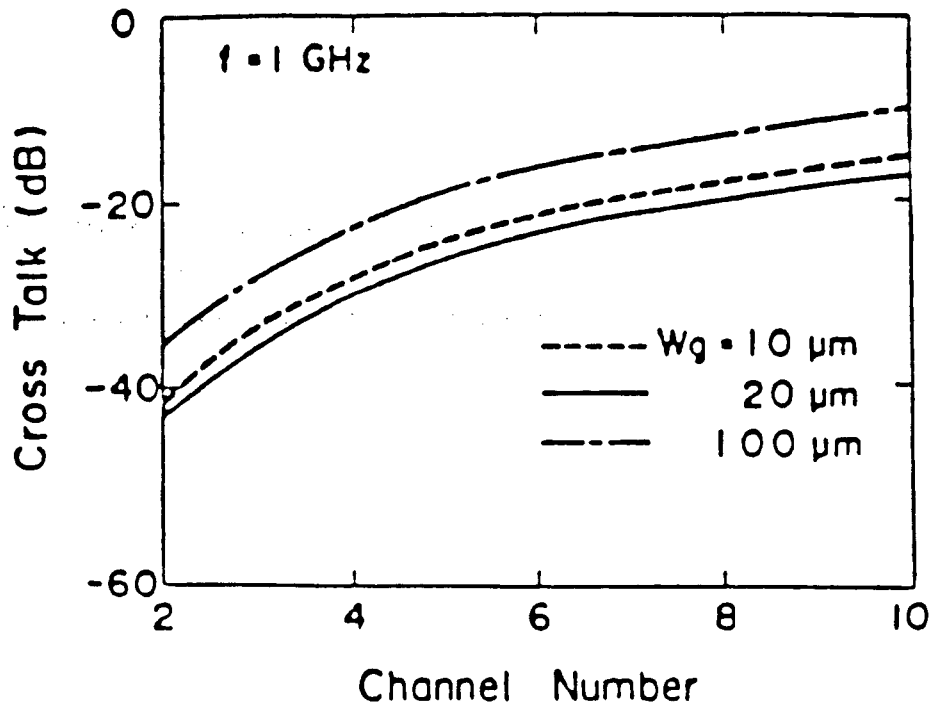


Fig. 31. Simulation of crosstalk versus channel number for GaAs MMIC technology (After Ref. 24).

The monolithic optoelectronic switching systems have their own drawbacks, too. They need electrical-to-optical conversion at the inputs. Also, the technology of monolithic optoelectronic integration is still in its infancy.

8.2 TECHNOLOGY NEEDED FOR MONOLITHIC OPTOELECTRONIC SWITCHING

Monolithic integration of optoelectronic devices is important in fully exploiting the system advantages of optoelectronic switching. Monolithic integration not only offers im-

proved performance of optical and electronic semiconductor devices but also enables developments of new devices. Technologies such as integrating lasers, photoconductors, and transistors on the same chip, processing techniques and material advancements are the fundamental requirements for monolithic optoelectronic switch matrices.

To be monolithically integrated with other elements, the laser diodes are required to have a low threshold current as well as a low sensitivity of threshold current to temperature, a capability of stable single-mode operation, and a high modulation speed. The low threshold current results from low power consumption requirement within the optoelectronic integrated circuit (OEIC) chips. This can be achieved by using quantum well laser structures. A single quantum well laser can have a threshold current as low as 2.5 mA [66].

For optical signal detection, a planar structure photodetector is desirable for monolithic integration with other electronic circuits. Several possibilities have been proposed. These include photoconductors, FETs, and metal-semiconductor-metal photodiodes. It has been shown that modulation doped AlGaAs/GaAs photoconductors [67] have structures that are simple and planar as well as capable of being compatible with electronic devices, particularly FET amplifiers. This feature is very important to OEIC fabrication.

For signal amplification, the well developed AlGaAs/GaAs MESFETs can be extensively applied to OEIC fabrication.

In regard to integrated structure, there are two basic structures for monolithically integrating optoelectronic elements: vertical and horizontal. In a vertical structure, epitaxial structures for both electronic and optical devices are sequentially grown on a conductive substrate with an insulating layer to isolate two devices electrically. In a horizontal structure, the optoelectronic and electronic device structures are formed horizontally on a semi-insulating substrate. The horizontal structure is preferred for OEIC because it offers lower capacitive couplings between the devices.

Because an optoelectronic device has a thickness ($5\text{ }\mu\text{m}$ - $10\text{ }\mu\text{m}$) much larger than that of the electronic devices, the processing sequence required to fabricate these devices on the same substrate is very crucial. A general problem encountered is reproducibility in processing. Several techniques have been proposed to avoid this problem [68-73].

The materials for both the substrate and epitaxial layer are very important in OEIC fabrication. The substrate must have low densities of dislocation and defects and a high purity. High quality optical epitaxial layers with high uniformity and reproducibility can be grown by molecular beam epitaxy (MBE) [74] and the metal organic chemical vapor deposition (MOCVD) [75].

8.3 FUTURE OPTOELECTRONIC INTEGRATED CIRCUIT TECHNOLOGY

The technology of OEIC has progressed very rapidly in recent years. Basic circuits operating at several gigahertz, such as laser/driver optical sources and photoconductor/amplifier receivers, have been demonstrated. Monolithic optoelectronic integration will become more important as the system requirements emerges toward higher performance, particularly in high switching speed. Future technology must not only refine existing technology but also explore novel functions and structures. The multi-quantum well structure (MQW) approach has proven to have the most promise. The MQW offers very low laser threshold currents (sub-mA), high modulation speed (multi-gigahertz operation), and high reliability. Also, its structure and fabrication procedure match with electronic devices. It is predicted that integrated devices, which include laser diodes and photodetectors, based on the MQW structure will be the leading technology for future optoelectronic switching systems.

Chapter 9

CONCLUSIONS AND RECOMMENDATIONS

9.1 CONCLUSIONS

Optoelectronic switching for SS-TDMA applications has been studied. The study includes a literature search, a study of system requirements, an analysis of switching architectures, a study of system components, switch model optimization, and a discussion of system advantages of optoelectronic switching.

Literature Search- A literature search indicated that optoelectronic devices have been extensively studied during the past ten years; however, system concepts and architectures in optoelectronic switching have not attracted adequate attention.

System Requirements for SS-TDMA -

- Dynamic interconnectivity between the uplink and downlink beams.
- Capability of one-to-one, one-to-many, and broadcasting connections.
- Switch size of 20x20 with expandability to 100x100.
- High switching speed (10 ns), low power consumption, low crosstalk, high isolation, and small physical size.
- Long lifetime (at least 10 years).
- Redundancy embedded in the switch.
- Ability to withstand outside perturbations.

GaAs wideband/broadband switching technology - GaAs FETs switch matrices satisfactorily meet the switching speed, isolation, and insertion loss requirements of an IF switch matrix. However, crosstalk is a problem for monolithic GaAs switch matrices.

Optoelectronic switching architectures - Among the four switching architectures studied, the power-divided and crossbar switching architectures are good candidates for SS-TDMA IF switch applications.

System components - System components for optoelectronic switching include lasers, fiber couplers, and photodetectors. AlGaAs/GaAs lasers were selected as the optical sources because of their high reliability, long lifetime, and low cost. Fiber couplers and optical waveguides can be used for optical signal distribution in hybrid integration and monolithic integration switch matrices, respectively. Photoconductor arrays are recommended for optical signal detection because of their low power consumption and compatibility with electronic devices.

Switch models and optimization - Three switch models representing discrete component, hybrid integration, and monolithic integration switch matrices have been proposed. The discrete component switch model is useful for demonstrating the optoelectronic switching concept, but hybrid and monolithic integration switch models are the recommended candidates for SS-TDMA applications. The monolithic integration switch model is much better than hybrid integration switch model in performance. However, because the OEIC technology is not yet mature, only a small switch matrix has been demonstrated.

System advantages and disadvantages of optoelectronic switching - The advantages are: low crosstalk, high isolation, small physical size, and low power dissipation. The disadvantages are: need of an electrical-to-optical conversion at input ends and unavailability of large-scale monolithic integration at present time.

The multi-quantum well structure approach is predicted to be the leading technology for future optoelectronic switching systems.

9.2 RECOMMENDATIONS

The following near term development and long term research are recommended as a result of this study:

Near term development - Experimental demonstration of a 4x4 optoelectronic switch matrix using hybrid or monolithic integration. The experimental data can be used to verify and refine system performance models.

Long term research -

- Research on material properties; trying to achieve subpicosecond response time in photodetectors.
- Research on techniques to produce a stable and high-frequency modulated laser output without excessive noise.
- Research on novel integration technology to produce high operation-frequency, high reliability, and low cost monolithic optoelectronic switches.

Chapter 10

REFERENCES

1. "Spacecraft IF switch matrix for advanced technology communication satellite systems," Final Report: Proof-of-Concept Model, NASA CR-168175, July 1983.
2. "30/20 GHz satellite communications programs," NASA Technology Development, November 1981.
3. "Spacecraft switch matrix for wideband service applications in 30/20 GHz communication satellite systems," Task II: Switch Matrix Design Study Using 1987 Technology, Final Report, NASA 1-11-F-1-T2, November 1981.
4. R. A. Gaspari and H. H. Yee, "Microwave GaAs FET switching," IEEE Microwave Symp. Dig., pp. 58-60, 1978.
5. W. Fabian, J. L. Vorhaus, J. E. Curtis, Sr., and P. Ng, "Dual-gate GaAs FET switches," Res. Abstracts: GaAs Integrated Circuit Symp. (Lake Tahoe, NV) 1979.
6. R. L. Van Tuyl and C. A. Liechti, "High speed integrated logic with GaAs MESFET," IEEE J. Solid-State Circuits, vol. SC-9, pp. 269-276, Oct. 1974.
7. A. Gopinath and J. B. Rankin, "GaAs FET RF switches," IEEE Tran. Electron Devices, vol. ED-32, pp. 1272-1278, July 1985.
8. S. A. Roosild, "DARPA GaAs plans and pilot production line project," Proc. IEEE Int. Conf. Computer Design: VLSI, pp. 251-257, Oct. 1984.
9. N. Yokoyama et al., "A GaAs 1K static RAM using tungsten silicide gate self-aligned technology," IEEE J. Solid State Circuits, vol. SC-18, pp. 520-524, Oct. 1983.
10. T. T. Vu et al., "A gallium arsenide SDFL gate array with on-chip ram," IEEE J. Solid State Circuits, vol. SC-19, pp. 10-22, Jan. 1984.
11. N. Yokoyama et al., "A 3 ns GaAs 4k x 1b SRAM," IEEE ISSCC, Paper WAM 3.3, Feb. 1984.
12. N. Mirayaman et al., "A GaAs 4kB SRAM with direct coupled FET logic," IEEE ISSCC, Paper WAM 3.4, Feb. 1984.
13. M. Abe, T. Mimura, N. Yokoyama, and H. Ishikawa, "New technology towards GaAs LSI/VLSI for computer applications," IEEE Trans. Electron Devices, vol. D-29, pp. 1088-1094, July 1982.
14. R. Zuleeg, "Is GaAs ready for VLSI?" J. Electr. and Electron. Eng. Aust., vol. 4, pp. 263-265, Dec. 1984.
15. T. E. Bell, "Japan reaches beyond silicon," IEEE Spectrum, vol. 22, pp. 46-52, Oct. 1985.
16. S. F. Su, L. Jou, S. Y. Lin, and J. Lenart, "A study of GaAs logic," GTE Tech. Report, TR85-260.4, Oct. 1985.

17. N. Yokoyama, T. Mimura, and M. Fukuta, "Planar GaAs MOSFET integrated logic," IEEE Trans. Electron Devices, vol. ED-27, pp. 1124-1128, June 1980.
18. R. C. Eden, B. M. Welch, R. Zucca, and S. I. Long, "The prospects for ultrahigh-speed VLSI GaAs digital logic," IEEE J. Solid State Circuits, vol. SC-14, pp. 221-239, April 1979.
19. B. M. Welch, Y. D. Shen, R. Zucca, R. C. Eden, and S. I. Long, "LSI processing technology for planar GaAs integrated circuits," IEEE Trans. Electron Devices, vol. ED-27, pp. 1116-1124, June 1980.
20. N. Kato, T. Mizutani, S. Ishida, and M. Ohmori, "Electron-beam fabrication of submicrometer gates for a GaAs MESFET logic," IEEE Trans. Electron Devices, vol. ED-27, pp. 1098-1101, June 1980.
21. N. Yokoyama et al., "TiW silicide gate self-alignment technology for ultra-high-speed GaAs MESFET LSI/VLSIs," IEEE Trans. Electron Devices, vol. ED-29, pp. 1541-1547, Oct. 1982.
22. H. Onodera et al., "A high-transconductance self-aligned GaAs MESFET fabricated by through-AIN implantation," IEEE Trans. Electron Devices, vol. ED-31, pp. 1808-1813, Dec. 1984.
23. Z. Ravnoy et al., "Vertical FETs in GaAs," IEEE Electron Device Lett., vol. EDL-5, pp. 228-230, July 1984.
24. Y. Nakayama et al., "A GaAs data switching IC for gigabits per second communication systems," IEEE J. Solid State Circuits, vol. SC-21, pp. 157-161, Feb. 1986.
25. Y. Tajima, W. Titus, R. Mozzi, and A. Morris, "Broadband GaAs FET 2 x 1 switches," 1984 GaAs IC Symp., Tech. Dig., pp. 81-84, Oct. 1984.
26. R. I. MacDonald and E. M. Hara, "Optoelectronic broadband switching array," Electron. Lett., vol. 14, pp. 502-503, Aug. 1978.
27. S. F. Su, L. Jou, and J. Lenart, "Bibliographies - Optoelectronic switching, optical switching, and electronic switching (discrete and monolithic semiconductors)," GTE Internal Report, May 1986.
28. R. I. MacDonald, D. K. W. Lam, R. H. Hum, and J. P. Noad, "Monolithic array of optoelectronic broadband switches," IEEE J. Solid State Ckt., vol. SC-19, pp. 219-223, April 1984.
29. E. H. Hara, "Optoelectronic switching," SPIE Proc., vol. 517, pp. 234-241, 1984.
30. D. K. W. Lam and R. I. MacDonald, "Fast optoelectronic crosspoint electrical switching of GaAs photodetectors," IEEE Electron Device Lett., vol. EDL-5, pp. 1-3, Jan. 1984.
31. A. M. Johnson and D. H. Auston, "Microwave switching by picosecond photoconductivity," IEEE J. Quantum Electron., vol. QE-11, pp. 283-287, June 1975.
32. R. A. Kiehl, "An avalanching optoelectronic microwave switch," IEEE Trans. Microwave Theory Tech., vol. MTT-27, pp. 533-539, May 1979.
33. J. C. Gammel and J. M. Ballantyne, "An integrated photoconductive detector and waveguide structure," Appl. Phys. Lett., vol. 36, pp. 149-151, Jan. 1980.

34. C. Baack, G. Elze, and G. Wolf, "GaAs MESFET: a high-speed optical detector," *Electron. Lett.*, vol. 13, pp. 193-194, 1977.
35. C. W. Slayman and L. Figueroa, "Frequency and pulse response of a novel high speed interdigital surface photoconductor (IDPC)," *IEEE Electron. Device Lett.*, vol. EDL-2, pp. 112-113, May 1981.
36. H. J. Klein et al., "High speed $\text{Ga}_{0.7}\text{In}_{0.3}\text{As}$ photoconductive detector for picosecond light pulses," *Electron. Lett.*, vol. 17, pp. 421-422, June 1981.
37. J. C. Gammel, G. M. Metze, and J. M. Ballantyne, "A photoconductive detector for high-speed fiber communication," *IEEE Trans. Electron Devices*, vol. ED-28, pp. 841-849, July 1981.
38. C. H. Lee and V. K. Mathur, "Picosecond photoconductivity and its applications," *IEEE J. Quantum Electron.*, vol. QE-17, pp. 2098-2112, Oct. 1981.
39. A. G. Foyt, F. J. Loenberger, and R. C. Williamson, "Picosecond InP optoelectronic switches," *Appl. Phys. Lett.*, vol. 40, pp. 447-449, March 1982.
40. E. H. Hara and R. I. MacDonald, "Characteristics of a photoconductive detector as an optoelectronic switch," *IEEE J. Quantum Electron.*, vol. QE-19, pp. 101-105, Jan. 1983.
41. C. Y. Chen et al., "Interdigitated $\text{Al}_{0.8}\text{In}_{0.2}\text{As}/\text{Ga}_{0.7}\text{In}_{0.3}\text{As}$ photoconductive detectors," *Appl. Phys. Lett.*, vol. 44, pp. 99-101, Jan. 1984.
42. N. Uesugi, S. Machida, and T. Kimura, "4x8 optoelectronic matrix switch equipment using InGaAs/InP heterojunction switching photodiodes," *Opt. Quantum Electron.*, vol. 15, pp. 217-224, May 1983.
43. O. Wada, T. Sakurai, and T. Nakayami, "Recent progress in optoelectronic integrated circuits," *IEEE J. Quantum Electron.*, vol. QE-22, pp. 805-821, June 1986.
44. E. H. Hara et al., "A high speed optoelectronic matrix switch using heterojunction switching diodes," *IEEE J. Quantum Electron.*, vol. QE-17, pp. 1539-1546, Aug. 1981.
45. E. H. Hara, R. I. MacDonald, and R. H. Hum, "Application of the optoelectronic matrix switch to communication systems," *IEEE 1981 Nat. Telecommun. Conf.*, vol. 2, pp. C1.2/1-4, Nov. 1981.
46. R. I. MacDonald, "Optoelectronic switching in digital networks," *IEEE J. Sel. Areas Commun.*, vol. SAC-3, no. 2, pp. 336-344, March 1985.
47. A. Neyer, "Electro-optic x-switch using single-mode Ti:LiNbO_3 channel waveguides," *Electron. Lett.*, vol. 19, pp. 553-554, July 1983.
48. R. V. Schmidt and H. Kogelnik, "Electrooptically switched coupler with stepped $\Delta\beta$ -reversal using Ti-diffused LiNbO_3 waveguides," *Appl. Phys. Lett.*, vol. 28, pp. 503-506, May 1976.
49. R. C. Alferness, "Guided-wave devices for optical communication," *IEEE J. Quantum Electron.*, vol. QE-17, pp. 946-959, June 1981.
50. V. Ramaswamy, M. Divino, and R. K. Standley, "A balanced bridge modulator switch," *Appl. Phys. Lett.*, vol. 32, pp. 644-646, 1978.

51. M. Minakota, "Efficient LiNbO_3 balanced bridge modulator/switch with ion etched slot," *Appl. Phys. Lett.*, vol. 35, pp. 40-42, 1979.
52. G. T. Sincerbox and G. Roosen, "Opto-optical light deflection," *Appl. Opt.*, vol. 22, pp. 690-697, March 1983.
53. G. Roosen and M. T. Plantegenest, "Transient hologram in a photorefractive material as a high capacity optical switching devices," *Ferroelectrics*, vol. 56, pp. 137-140, April 1984.
54. C. B. Su et al., "12-5 GHz direct modulation bandwidth of vapor phase regrown $1.3\ \mu\text{m}$ InGaAsP buried structure lasers," *Appl. Phys. Lett.*, vol. 46, pp. 344-346, 1985.
55. J. E. Bowers, et al., "High-frequency constricted mesa lasers," *Appl. Phys. Lett.*, vol. 47, pp. 78-80, 1985.
56. C. M. Gee and G. D. Thurmond, "Wideband travelling-wave electro-optic modulator," *Proc. SPIE*, vol. 477, pp. 17-22, 1984.
57. H. Kanbe, et al., "InGaAs avalanche photodiode with InP p-n junction", *Electron Lett.*, vol. 16, pp. 163-165, Feb. 1980.
58. J. C. Campbell, et al., "A high-speed InP/InGaAs avalanche photodiode exhibiting a gain-bandwidth product of 60 GHz," *IOOC-ECOC 85, Tech. Digest. 3*, p. 65, 1985.
59. S. Y. Wang, et al., "20-GHz bandwidth GaAs photodiode," *Appl. Phys. Lett.*, vol. 42, pp. 190-191, Jan. 1983.
60. S. Y. Wang and D. M. Bloom, "100 GHz bandwidth planar GaAs Schottky photodiode," *Electron. Lett.*, vol. 19, pp. 554-555, July 1983.
61. F. J. Leonberger and V. Diadiuk, "High-speed InP-based photodetectors," *IEDM 83, Tech Digest*, pp. 460-463, 1983.
62. S. R. Forrest, "The sensitivity of photoconductor receivers for long-wavelength optical communications," *J. Lightwave Tech.*, vol. LT-3, pp. 347-360, April 1985.
63. E. H. Hara and R. I. MacDonald, "Characteristics of a photoconductive detector as an optoelectronic switch," *IEEE J. Quantum Electron.*, vol. QE-19, pp. 101-105, Jan. 1983.
64. C. W. Slayman and L. Figueroa, "Frequency and pulse response of a novel high speed interdigitated surface photoconductor," *IEEE Electron Device Lett.*, vol. EDL-2, pp. 112-113, May 1981.
65. C. Y. Chen, et al., "2-Gb/s sensitivity of a $\text{Ga}_{0.47}\text{In}_{0.53}\text{As}$ photoconductive detector/GaAs effect transistor hybrid photoreceiver," *Appl. Phys. Lett.*, vol. 46, pp. 379-381, Feb. 1985.
66. W. T. Tsang, et al., "Ultra-low threshold, graded-index waveguide, separate confinement, CW buried-heterostructure lasers," *Electron Lett.*, vol. 18, pp. 845-847, Sept. 1982.
67. V. Diadiuk and S. H. Groves, "Lateral photodetectors on semi-insulating InGaAs and InP," *Appl. Phys. Lett.*, vol. 46, pp. 157-158, 1985.
68. R. M. Kolbas, et al., "Planar monolithic integration of a photodiode and a GaAs preamplifier," *Appl. Phys. Lett.*, vol. 43, pp. 821-823, 1983.

69. C. S. Hong, et al., "Integrated quantum-well-laser transmitter compatible with ion-implanted circuits," *Electron. Lett.*, vol. 20, pp. 733-735, 1985.
70. A. S. H. Liao, et al., "A planar embedded InGaAs photodiode PIN-FET receivers, using selective vapor phase epitaxy and ion implantation technique," *Tech. Dig., IEDM*, Washington, DC, pp. 478-481, 1983.
71. M. E. Kim, et al., "GaAs/GaAlAs selective MOCVD epitaxy and planar ion-implantation technique for complex integrated optoelectronic circuit applications," *IEEE Electron Device Lett.*, vol. EDL-5, pp. 306-309, 1984.
72. S. Miura, et al., "Monolithic integration of a pin photodiode and a field-effect transistor using a new fabrication technique - Graded-step process," *Appl. Phys. Lett.*, vol. 46, pp. 389-391, 1985.
73. O. Wada, et al., "A new fabrication technique for optoelectronic integrated circuits - the graded-step process - applied to the fabrication of AlGaAs/GaAs PIN/FET and PIN/amplifier photoreceivers," *J. Electrochem. Soc.*, vol. 132, pp. 1996-2002, 1985.
74. W. T. Tsang, "Heterostructure semiconductor lasers prepared by molecular beam epitaxy," *IEEE J. Quantum Electron.*, vol. QE-20, pp. 1119-1132, 1984.
75. G. B. Strinifellow, "Organometalic vapor phase epitaxial growth of III-V semiconductors," *Semiconductors and Semimetals*, R. K. Willardson and A. C. Beer, ed., vol. 22, Part A, W. T. Tsang, ed., Orlando, FL; Academic, 1985, ch. 3.